Numerical hydrodynamics in general relativity

José A. Font
Max-Planck-Institut für Astrophysik
Karl-Schwarzshild-Str. 1
D-85740 Garching, Germany

Abstract

The current status of numerical solutions for the equations of ideal general relativistic hydrodynamics is reviewed. Different formulations of the equations are presented, with special mention to conservative and hyperbolic formulations well-adapted to advanced numerical methods. A representative sample of available numerical schemes is discussed and particular emphasis is paid on solution procedures based on schemes exploiting the characteristic structure of the equations through linearized Riemann solvers. A comprehensive summary of relevant astrophysical simulations in strong gravitational fields, including gravitational collapse, accretion onto black holes and evolution of neutron stars, is also presented.

1 Introduction

The description of important areas of modern astronomy such as high-energy astrophysics or gravitational wave astronomy, requires General Relativity. High energy radiation is often emitted by highly relativistic events in regions of strong gravitational fields near compact objects such as neutron stars or black holes. The standard model for powering radio galaxies and their associated relativistic jets is the magnetic extraction of energy from spinning black holes through the Blandford-Znajek mechanism [24, 162]. The recent discovery of kHz quasi-periodic oscillations in low-mass X-ray binaries extends the frequency range over which these oscillations occur into timescales associated with the innermost regions of accretion disks (see, e.g. [195]). Scenarios involving explosive collapse of very massive stars ($\approx 30 M_{\odot}$) to a black hole (the so-called collapsar and hypernova models) or coalescing compact binaries containing two neutron stars or a neutron star and a black hole have been proposed as possible candidates to power γ-ray bursts [147, 139, 211, 148]. In addition, coalescing neutron star binaries are among the strongest emitters of gravitational radiation and they

constitute one of the main targets for the new generation of gravitational wave detectors going online worldwide in the next few years [194].

A powerful way to improve our understanding of such events is through accurate, large scale, three-dimensional numerical simulations. In the most general case, the equations governing the dynamics of those systems are an intrincated, coupled system of time-dependent partial differential equations, comprising the (general) relativistic (magneto) hydrodynamic equations and the Einstein gravitational field equations. In many cases, the number of equations must be even augmented to account for non-adiabatic processes, as, e.g., radiative transfer or sophisticated microphysics (realistic equations of state for nuclear matter, nuclear physics, magnetic fields, etc.).

Nevertheless, in some astrophysical situations of interest, as e.g., accretion of matter on to compact objects, the 'test-fluid' approximation is commonly adopted and suffices to get an accurate description. In this approximation the fluid self-gravity is neglected in comparison to the *background* gravitational field. The core assumption is then that the mass μ, of the accreting fluid, is much smaller than the mass of the compact object M, i.e., $\mu << M$. For instance, a black hole accreting matter at the Eddington rate $\dot{M}_{Edd} \equiv L_{Edd}/c^2 = 1.4\times10^{17} M/M_{\odot}[gs^{-1}]$ would need about 10^8 years to double its mass, which certainly validates the assumption. Additionally, a description employing ideal hydrodynamics (i.e., with the stress-energy tensor being that of a perfect fluid), is also a fairly standard choice in numerical astrophysics.

It is the main aim of this review to summarize the existing efforts to solve the equations of (ideal) general relativistic hydrodynamics by numerical means. For this purpose, the most relevant numerical schemes will be presented in some detail. Furthermore, relevant applications in a number of different astrophysical systems, including gravitational collapse, accretion on to compact objects and hydrodynamical evolution of neutron stars, will be also summarized here. Numerical simulations of strong-field scenarios employing Newtonian gravity and hydrodynamics, as well as possible post-Newtonian extensions, have received considerable attention in the literature and will not be covered here. Interested readers are addressed to e.g. [132, 136, 167] and references therein.

The organization of the paper is as follows: Section 2 presents the equations of general relativistic hydrodynamics, summarizing the most relevant theoretical formulations which, in turn, have driven, to some extent, the development of numerical algorithms for their solution. Section 3 is mainly devoted to describe numerical schemes specifically designed for non-linear hyperbolic systems. Hence, particular emphasis will be paid on conservative high-resolution shock-capturing methods based on linearized Riemann solvers. Alternative schemes such as smoothed particle hydrodynamics (SPH) and (pseudo) spectral methods will be also briefly discussed. Section 4 summarizes a comprehensive sample of hydrodynamical simulations in strong-field general relativistic astrophysics.

Geometrized units ($G = c = 1$) are used throughout the paper except where explicitly indicated as well as the metric conventions of [129]. Greek (Latin)

indices run from 0 to 3 (1 to 3).

2 Equations of general relativistic hydrodynamics

The general relativistic hydrodynamic equations consist of the local conservation laws of the stress-energy tensor, $T^{\mu\nu}$ (the Bianchi identities) and of the matter current density, J^μ (the continuity equation)

$$\nabla_\mu T^{\mu\nu} = 0, \tag{1}$$

$$\nabla_\mu J^\mu = 0. \tag{2}$$

As usual ∇_μ stands for the covariant derivative associated to the four-dimensional spacetime metric, $g_{\mu\nu}$. The density current is given by $J^\mu = \rho u^\mu$, u^μ representing the fluid 4-velocity and ρ the rest-mass density in a locally inertial reference frame.

The stress-energy tensor for a non-perfect fluid is defined as

$$T^{\mu\nu} = \rho(1+\varepsilon)u^\mu u^\nu + (p-\zeta\theta)h^{\mu\nu} - 2\eta\sigma^{\mu\nu} + q^\mu u^\nu + q^\nu u^\mu \tag{3}$$

where ε is the rest frame specific internal energy density of the fluid, p is the pressure and $h^{\mu\nu}$ is the spatial projection tensor $h^{\mu\nu} = u^\mu u^\nu + g^{\mu\nu}$. In addition, η and ζ are the shear and bulk viscosities. The expansion, θ, describing the divergence or convergence of the fluid world lines is defined as $\theta = \nabla_\mu u^\mu$. The symmetric, trace-free, and spatial shear tensor $\sigma^{\mu\nu}$ is defined by

$$\sigma^{\mu\nu} = \frac{1}{2}(\nabla_\alpha u^\mu h^{\alpha\nu} + \nabla_\alpha u^\nu h^{\alpha\mu}) - \frac{1}{3}\theta h^{\mu\nu}, \tag{4}$$

and, finally, q^μ is the energy flux vector.

In the following we will neglect non-adiabatic effects, such as viscosity or heat transfer, assuming the stress-energy tensor to be that of a perfect fluid

$$T^{\mu\nu} = \rho h u^\mu u^\nu + p g^{\mu\nu}, \tag{5}$$

where we have introduced the relativistic specific enthalpy, h, defined by

$$h = 1 + \varepsilon + \frac{p}{\rho}. \tag{6}$$

Introducing an explicit coordinate chart (x^0, x^i) the previous conservation equations read

$$\frac{\partial}{\partial x^\mu}\sqrt{-g}J^\mu = 0\,, \tag{7}$$

$$\frac{\partial}{\partial x^\mu}\sqrt{-g}T^{\mu\nu} = -\sqrt{-g}\Gamma^\nu_{\mu\lambda}T^{\mu\lambda}\,, \tag{8}$$

where the scalar x^0 represents a foliation of the spacetime with hypersurfaces (coordinatized by x^i). Additionally, $\sqrt{-g}$ is the volume element associated with the 4-metric, with $g = \det(g_{\mu\nu})$, and $\Gamma^{\nu}_{\mu\lambda}$ are the 4-dimensional Christoffel symbols.

The system formed by the equations of motion (1) and the continuity equation (2) must be supplemented with an equation of state (EOS) relating some fundamental thermodynamical quantities. In general, the EOS takes the form

$$p = p(\rho, \varepsilon). \tag{9}$$

In the 'test-fluid' approximation, where the fluid self-gravity is neglected, the dynamics of the system is completely governed by Eqs. (1) and (2), together with the EOS (9). In those situations where such approximation does not hold, the previous equations must be solved in conjunction with the Einstein gravitational field equations

$$G^{\mu\nu} = 8\pi T^{\mu\nu} \tag{10}$$

which describe the evolution of a dynamical spacetime. The formulation of the Einstein equations as an initial value (Cauchy) problem, in the presence of matter fields, adopting the so-called 3+1 decomposition of the spacetime [9] can be found in, e.g., [216]. Given a choice of gauge, the Einstein equations in the 3+1 formalism [9] split into evolution equations for the 3–metric γ_{ij} and the extrinsic curvature K_{ij} and constraint equations, the Hamiltonian and momentum constraints, that must be satisfied at every time slice. Alternatively, a characteristic initial value problem formulation of the Einstein equations was developed by Bondi, van der Burg and Metzner [32] and Sachs [168]. A recent review of the characteristic formulation is presented in [209].

Traditionally, most of the approaches for numerical integrations of the general relativistic hydrodynamic equations have adopted spacelike foliations of the spacetime, within the 3+1 formulation. Recently, however, covariant forms of these equations, well suited for advanced numerical methods, have also been developed. This is reviewed next in a chronological way.

2.1 Spacelike (3+1) approaches

In the 3+1 (ADM) formulation [9], spacetime is foliated into a set of non-intersecting spacelike hypersurfaces. There are two kinematic variables describing the evolution between these surfaces: the lapse function α, which describes the rate of advance of time along a timelike unit vector n^μ normal to a surface, and the spacelike shift vector β^i that describes the motion of coordinates within a surface.

The line element is written as

$$ds^2 = -(\alpha^2 - \beta_i\beta^i)dx^0dx^0 + 2\beta_i dx^i dx^0 + \gamma_{ij}dx^i dx^j, \tag{11}$$

where γ_{ij} is the 3–metric induced on each spacelike slice.

2.1.1 May and White

The pioneering numerical work in general relativistic hydrodynamics dates back to the one-dimensional gravitational collapse code of May and White [118, 119]. Building on theoretical work by Misner and Sharp [128] May and White developed a numerical code to solve the evolution equations describing adiabatic spherical collapse in general relativity. This code was based on a Lagrangian finite difference scheme, in which the coordinates are co-moving with the fluid. Artificial viscosity terms were included in the equations to damp the spurious numerical oscillations caused by the presence of shock waves in the flow solution. May and White's formulation became the starting point of a large number of numerical investigations in subsequent years and, hence, it is worth describing its main features in some detail.

For a spherically symmetric spacetime the line element can be written as

$$ds^2 = -a^2(m,t)dt^2 + b^2(m,t)dm^2 + R^2(m,t)(d\theta^2 + \sin^2\theta d\phi^2) \tag{12}$$

m being a radial (Lagrangian) coordinate, indicating the total rest-mass enclosed inside the circumference $2\pi R(m,t)$.

The co-moving character of the coordinates leads, for a perfect fluid, to a stress-energy tensor of the form:

$$T^1_1 = T^2_2 = T^3_3 = -p, \tag{13}$$

$$T^0_0 = (1+\varepsilon)\rho, \tag{14}$$

$$T^\mu_\nu = 0 \quad \text{if} \quad \mu \neq \nu. \tag{15}$$

In these coordinates the local conservation equation for the baryonic mass, Eq. (2), can be easily integrated

$$b = \frac{1}{4\pi\rho R^2}. \tag{16}$$

The gravitational field equations, Eq. (10), and the equations of motion, Eq. (1), reduce to the following quasi-linear system of partial differential equations (see also [128]):

$$\frac{\partial p}{\partial m} + \frac{1}{a}\frac{\partial a}{\partial m}\rho h = 0, \tag{17}$$

$$\frac{\partial \varepsilon}{\partial t} + p\frac{\partial}{\partial t}\left(\frac{1}{\rho}\right) = 0, \tag{18}$$

$$\frac{\partial u}{\partial t} = -a\left(4\pi\frac{\partial p}{\partial m}R^2\frac{\Gamma}{h} + \frac{M}{R^2} + 4\pi pR\right), \tag{19}$$

$$\frac{1}{\rho R^2}\frac{\partial \rho R^2}{\partial t} = -a\frac{\partial u/\partial m}{\partial R/\partial m}, \tag{20}$$

with the definitions $u = \frac{1}{a}\frac{\partial R}{\partial t}$ and $\Gamma = \frac{1}{b}\frac{\partial R}{\partial m}$, satisfying $\Gamma^2 = 1 - u^2 - \frac{2M}{R}$. Additionally,

$$M = \int_0^m 4\pi R^2 \rho(1+\varepsilon)\frac{\partial R}{\partial m}dm, \tag{21}$$

represents the total mass interior to radius m at time t. The final system is closed with an EOS of the form (9).

Codes based on the original formulation of May and White and on later versions (e.g., [198]) have been used in many supernova and neutron star collapse non-linear calculations (see, e.g., [127, 191] and references therein), as well as in perturbative computations of spherically symmetric gravitational collapse employing the linearized Einstein theory [172, 174, 173]. In Section 4.1.1 some of these simulations will be reviewed in detail. The Lagrangian character of May and White's code, together with other theoretical considerations concerning the particular coordinate gauge, has prevented its extension to multidimensional calculations.

2.1.2 Wilson

The use of Eulerian coordinates in multidimensional numerical relativistic hydrodynamics started with the pioneering work by Wilson [203]. Introducing the basic dynamical variables D, S_μ and E, representing the relativistic density, momenta and energy, respectively, defined as

$$D = \rho u^0, \qquad S_\mu = \rho h u_\mu u^0, \qquad E = \rho\varepsilon u^0, \tag{22}$$

the equations of motion in Wilson's formulation [203, 204] are:

$$\frac{1}{\sqrt{-g}}\frac{\partial}{\partial x^0}(D\sqrt{-g}) + \frac{1}{\sqrt{-g}}\frac{\partial}{\partial x^i}(DV^i\sqrt{-g}) = 0, \tag{23}$$

$$\frac{1}{\sqrt{-g}}\frac{\partial}{\partial x^0}(S_\mu\sqrt{-g}) + \frac{1}{\sqrt{-g}}\frac{\partial}{\partial x^i}(S_\mu V^i\sqrt{-g}) + \frac{\partial p}{\partial x^\mu} + \frac{1}{2}\frac{\partial g^{\alpha\beta}}{\partial x^\mu}\frac{S_\alpha S_\beta}{S^0} = 0, \tag{24}$$

$$\frac{\partial}{\partial x^0}(E\sqrt{-g}) + \frac{\partial}{\partial x^i}(EV^i\sqrt{-g}) + p\frac{\partial}{\partial x^\mu}(u^0 V^\mu\sqrt{-g}) = 0. \tag{25}$$

with the "transport velocity" given by $V^\mu = u^\mu/u^0$. Notice that the momentum density equation, Eq. (24), is only solved for the three spatial components, S_i, and S_0 is obtained through the 4-velocity normalization condition $u_\mu u^\mu = -1$.

A direct inspection of the system shows that the equations are written as a coupled set of advection equations. In doing so, this approach sidesteps an important guideline for the formulation of non-linear hyperbolic systems of equations, namely the preservation of their *conservation form*. This is a necessary

feature to guarantee correct evolution in regions of sharp entropy generation (i.e., shocks). As a consequence, some amount of numerical dissipation must be used to stabilize the solution across discontinuities. The first attempt to solve the equations of general relativistic hydrodynamics in the original Wilson's scheme [203] used a combination of finite difference upwind techniques with artificial viscosity terms. Such terms extended the classic treatment of shocks introduced by von Neumann and Richtmyer [200] into the relativistic regime (see Section 3.1.1).

Wilson's formulation has been widely used in hydrodynamical codes developed by a variety of research groups. Many different astrophysical scenarios were first investigated with these codes, including axisymmetric stellar core-collapse [135, 134, 138, 13, 188, 158, 57], accretion onto compact objects [84, 156], numerical cosmology [39, 40, 7] and, more recently, the coalescence and merge of neutron star binaries [207, 208]. This formalism has also been extensively employed, in the special relativistic limit, in numerical studies of heavy-ion collisions [206, 121]. In all these investigations, the original formulation of the hydrodynamic equations was slightly modified by re-defining the dynamical variables, Eq. (22), with the addition of a multiplicative α factor and the introduction of the Lorentz factor, $W \equiv \alpha u^0$ (the "relativistic gamma"):

$$D = \rho W, \qquad S_\mu = \rho h W u_\mu, \qquad E = \rho \varepsilon W. \tag{26}$$

As mentioned at the beginning of this section, to describe the evolution of self-gravitating matter fields coupled to the spacetime dynamics requires of a joint integration of the hydrodynamic equations and the gravitational field (Einstein) equations. Within Wilson's formulation, such a coupled evolution was first considered in collaboration with Smarr [204], building on a vacuum spacetime code specifically developed to investigate the head-on collision of two black holes [186]. The resulting code was axially symmetric and aimed to integrate the coupled system in the context of stellar core collapse [59]. More recently, fully dynamical evolutions of the spacetime and the hydrodynamics have been performed, within the Wilson approach, in studies of binary neutron star coalescence [207, 208]. In contrast to earlier approaches, where the full set of Einstein equations was discretised [59], the latter investigations dealt with a considerably reduced set of spacetime equations, by assuming the simplifying condition that the geometry is conformally flat at all times during an evolution. Within this approximation the field equations reduce to a set of five Poisson-like elliptic equations in flat spacetime for the lapse, the shift vector and the conformal factor.

Wilson's formulation showed some limitations to handle situations involving ultra relativistic flows, as first pointed out by Centrella and Wilson [40]. Norman and Winkler [143] performed a comprehensive numerical study of such formulation by means of special relativistic hydrodynamical simulations. Figure 1 reproduces a plot from [143] in which the relative error of the numerical

solution for the relativistic shock reflection problem – the heating of a cold gas which impacts at relativistic speeds with a solid wall and bounces back – is displayed as a function of the Lorentz factor, W, of the incoming gas. The source of the data is [40]. This figure shows that for Lorentz factors of $W \approx 2$ ($v \approx 0.86c$), the threshold of the ultra relativistic limit, the relative errors are between 5% and 7% (depending on the adiabatic exponent of the gas), showing a linear growth with W.

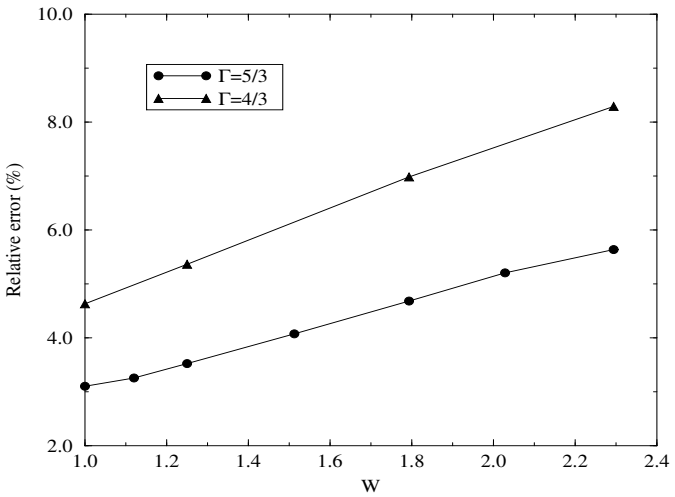

Figure 1: Results for the shock heating test of a cold, relativistically inflowing gas against a wall using the explicit Eulerian techniques of Centrella and Wilson [40]. Dependence of the relative errors versus the Lorentz factor W for two different values of the adiabatic index of the flow, $\Gamma = 4/3$ (triangles) and $\Gamma = 5/3$ (circles) gases. The data are from Centrella and Wilson [40] and the plot reproduces a similar one from Norman and Winkler [143].

Norman and Winkler [143] concluded that those large errors were mainly due to the way in which the artificial viscosity terms are included in the numerical scheme in Wilson's formulation. These terms, called collectively Q (see Section 3.1.1), are only added to the pressure terms in some cases, namely at the pressure gradient in the source of the momentum equation and at the divergence of the velocity in the source of the energy equation. However, [143] proposed to add the Q terms globally in order to consider the artificial viscosity as a real viscosity. Hence, the hydrodynamic equations should be rewritten for a modified stress-

energy tensor of the following form:

$$T^{\mu\nu} = \rho(1 + \varepsilon + (p+Q)/\rho)u^\mu u^\nu + (p+Q)g^{\mu\nu}. \tag{27}$$

In this way, in flat spacetime, the momentum equation takes the form:

$$\frac{\partial}{\partial x^0}[(\rho h + Q)W^2 V_j] + \frac{\partial}{\partial x^i}[(\rho h + Q)W^2 V_j V^i] + \frac{\partial (p+Q)}{\partial x^j} = 0. \tag{28}$$

In Wilson's formulation Q is omitted in the two terms containing the quantity ρh. In general Q is a non-linear function of the velocity and, hence, the quantity QW^2V in the momentum density of Eq. (28) is a highly non-linear function of the velocity and its derivatives. This fact, together with the explicit presence of the Lorentz factor in the convective terms of the hydrodynamic equations, as well as the pressure in the specific enthalpy, make the relativistic equations much more coupled than their Newtonian counterparts. As a result Norman and Winkler proposed the use of implicit schemes to describe more accurately such coupling. Their code, which incorporates an adaptive grid, reproduces very accurate results even for ultra relativistic flows with Lorentz factors of about 10 in one-dimensional, flat spacetime, simulations.

2.1.3 Valencia

In 1991 the *Valencia group* [112] presented a new formulation of the (Eulerian) general relativistic hydrodynamic equations. This formulation was aimed to take fundamental advantage of the hyperbolic and conservative character of the equations. Numerically, the hyperbolic and conservative nature of the relativistic Euler equations allows for the use of schemes based on the characteristic fields of the system, translating to relativistic hydrodynamics existing tools of classical fluid dynamics. This procedure departs from earlier approaches, most notably in avoiding the need for artificial dissipation terms to handle discontinuous solutions [204] as well as implicit schemes as proposed in [143].

A numerical scheme written in conservation form automatically guarantees the correct Rankine-Hugoniot (jump) conditions across discontinuities (the shock-capturing property). Writing the relativistic hydrodynamic equations as a system of conservation laws, identifying the suitable vector of unknowns and building up an approximate Riemann solver permitted the extension of state-of-the-art *high-resolution shock-capturing* (HRSC in the following) schemes from classical fluid dynamics into the realm of relativity [112].

Theoretical advances on the mathematical character of the relativistic hydrodynamic equations were achieved studying the special relativistic limit. In Minkowski spacetime, the hyperbolic character of relativistic (magneto) hydrodynamics was exhaustively studied by Anile and collaborators (see [5] and references therein) by applying Friedrichs' definition of hyperbolicity [69] to a

quasi-linear form of the system of hydrodynamic equations

$$\mathcal{A}^{\mu}(\mathbf{w})\frac{\partial \mathbf{w}}{\partial x^{\mu}} = 0, \tag{29}$$

where $\mathcal{A}^{\mu}$ are the Jacobian matrices of the system and $\mathbf{w}$ are a suitable set of *primitive* variables (see below). System (29) will be hyperbolic in the time-direction defined by the vector field ξ with $\xi_{\mu}\xi^{\mu} = -1$, if the following two conditions hold: (i) $\det(\mathcal{A}^{\mu}\xi_{\mu}) \neq 0$ and (ii) for any ζ such that $\zeta_{\mu}\xi^{\mu} = 0$, $\zeta_{\mu}\zeta^{\mu} = 1$, the eigenvalue problem $\mathcal{A}^{\mu}(\zeta_{\mu} - \lambda\xi_{\mu})\mathbf{r} = 0$ has only real eigenvalues $\{\lambda_n\}_{n=1,\cdots,5}$ and a complete set of right-eigenvectors $\{\mathbf{r}_n\}_{n=1,\cdots,5}$. Besides verifying the hyperbolic character of the relativistic hydrodynamic equations Anile and collaborators [5] obtained the explicit expressions for the eigenvalues and eigenvectors in the local rest frame, characterized by $u^{\mu} = \delta^{\mu}_0$. In Font et al [64] those calculations were extended to an arbitrary reference frame in which the motion of the fluid was described by the 4-velocity $u^{\mu} = W(1, v^i)$.

The extension to general relativity of the approach followed in [64] in special relativity was accomplished in [12]. We will refer to the formulation of the general relativistic hydrodynamic equations presented in [12] as *Valencia's formulation*. The choice of evolved variables (*conserved quantities*) in this formulation differs slightly from Wilson's formulation. It comprises the rest-mass density (D), the momentum density in the j-direction (S_j) and the total energy density (E), measured by a family of observers which are the natural extension (for a generic spacetime) of the Eulerian observers in classical fluid dynamics. Interested readers are addressed to [12] for their definition and geometrical foundations.

In terms of the *primitive variables* $\mathbf{w} = (\rho, v_i, \varepsilon)$ the conserved quantities are written as:

$$D = \rho W \tag{30}$$

$$S_j = \rho h W^2 v_j \tag{31}$$

$$E = \rho h W^2 - p \tag{32}$$

where the contravariant components $v^i = \gamma^{ij}v_j$ of the three-velocity are defined as

$$v^i = \frac{u^i}{\alpha u^0} + \frac{\beta^i}{\alpha} \tag{33}$$

and W is the relativistic Lorentz factor $W \equiv \alpha u^0 = (1 - v^2)^{-1/2}$ with $v^2 = \gamma_{ij}v^i v^j$.

With the previous choice of variables the equations can be written in *conservation* form. Strict conservation is only possible in flat spacetime. For curved spacetimes there exist source terms, coming from the spacetime geometry, which do not contain derivatives of stress-energy tensor components. More precisely,

the first-order flux-conservative hyperbolic system, well suited for numerical applications, reads:

$$\frac{1}{\sqrt{-g}}\left(\frac{\partial\sqrt{\gamma}\mathbf{U}(\mathbf{w})}{\partial x^0}+\frac{\partial\sqrt{-g}\mathbf{F}^i(\mathbf{w})}{\partial x^i}\right)=\mathbf{S}(\mathbf{w}) \tag{34}$$

with $g\equiv\det(g_{\mu\nu})$ satisfying $\sqrt{-g}=\alpha\sqrt{\gamma}$ with $\gamma\equiv\det(\gamma_{ij})$. The state vector is given by

$$\mathbf{U}(\mathbf{w})=(D,S_j,\tau) \tag{35}$$

with $\tau\equiv E-D$. The vector of fluxes is

$$\mathbf{F}^i(\mathbf{w})=\left(D\left(v^i-\frac{\beta^i}{\alpha}\right),S_j\left(v^i-\frac{\beta^i}{\alpha}\right)+p\delta^i_j,\tau\left(v^i-\frac{\beta^i}{\alpha}\right)+pv^i\right) \tag{36}$$

and the corresponding sources $\mathbf{S}(\mathbf{w})$ are

$$\mathbf{S}(\mathbf{w})=\left(0,T^{\mu\nu}\left(\frac{\partial g_{\nu j}}{\partial x^\mu}-\Gamma^\delta_{\nu\mu}g_{\delta j}\right),\alpha\left(T^{\mu 0}\frac{\partial \ln\alpha}{\partial x^\mu}-T^{\mu\nu}\Gamma^0_{\nu\mu}\right)\right). \tag{37}$$

The local characteristic structure of the previous system of equations was presented in [12]. The eigenvalues (characteristic speeds) of the corresponding Jacobian matrices are all real (but not distinct, one showing a threefold degeneracy) and a complete set of right-eigenvectors exists. System (34) satisfies, hence, the definition of hyperbolicity. As discussed in Section 3.1.2 below the knowledge of the spectral information is essential in order to construct HRSC schemes based on Riemann solvers. This information can be found in [12] (see also [67]).

The range of applications considered so far in general relativity employing this formulation is still small and mostly devoted to the study of accretion flows on to black holes (see Section 4.2.2 below). In the special relativistic limit this formulation is being successfully applied to model the evolution of (ultra) relativistic extragalactic jets (see, e.g. [116, 4]). The first numerical studies in general relativity were performed, in one spatial dimension, in [112], using a slightly different form of the equations. Preliminary investigations of gravitational stellar collapse were attempted by coupling Valencia's formulation to a hyperbolic formulation of the Einstein equations developed by [26]. Some discussion of these results can be found in [110, 25]. More recently, successful evolutions of fully dynamical spacetimes in the context of adiabatic spherically symmetric stellar core-collapse have been achieved [91, 165]. We will come back to these issues in Section 4.1.1 below.

Recently, a three-dimensional, Eulerian, general relativistic hydrodynamical code, evolving the coupled system of the Einstein and hydrodynamic equations has been developed [67]. The formulation of the hydrodynamic equations follows Valencia's approach. The code is constructed for a completely general spacetime metric based on a Cartesian coordinate system, with arbitrarily specifiable

lapse and shift conditions. In [67] the spectral decomposition (eigenvalues and right-eigenvectors) of the general relativistic hydrodynamic equations, valid for general spatial metrics, was derived, correcting earlier results of [12] for non-diagonal metrics. A complete set of left-eigenvectors has been recently presented by Ibáñez et al [89]. This information is summarized in Section 5.2.

The formulation of the coupled set of equations and the numerical code reported in [67] were used for the construction of the milestone code "GR3D" for the NASA Neutron Star Grand Challenge project. For a description of the project see the URL address `http://wugrav.wustl.edu/Relativ/nsgc.html`. A public domain version of the code has recently been released to the community. The source and documentation of this code can be downloaded at `http://wugrav.wustl.edu/Codes/GR3D`.

2.2 Covariant approaches

General (covariant) conservative formulations of the general relativistic hydrodynamic equations for ideal fluids, i.e., not restricted to spacelike foliations, have been derived in [56] and, more recently, in [152]. The *form invariance* of these approaches with respect to the nature of the spacetime foliation implies that existing work on highly specialized techniques for fluid dynamics (i.e. HRSC schemes) can be adopted straightforwardly. In the next two sections we describe them in some detail.

2.2.1 Eulderink and Mellema

Eulderink and Mellema [54, 56] first derived a covariant formulation of the general relativistic hydrodynamic equations taking special care, as in Valencia's formulation, of the conservative form of the system, with no derivatives of the dependent fluid variables appearing in the source terms. Additionally, this formulation is strongly tailored towards the use of a numerical method based on a generalization of Roe's approximate Riemann solver for the non-relativistic Euler equations in Cartesian coordinates [164]. Their procedure is specialized for a perfect fluid EOS, $p = (\Gamma - 1)\rho\varepsilon$, Γ being the (constant) adiabatic index of the fluid.

After the appropriate choice of the state vector variables the conservation laws, Eqs. (7) and (8), are re-written in flux-conservative form. The flow variables are expressed in terms of a parameter vector ω as:

$$\mathbf{F}^{\alpha} = \left(\left[K - \frac{\Gamma}{\Gamma - 1}\omega^4 \right] \omega^{\alpha}, \omega^{\alpha}\omega^{\beta} + K\omega^4 g^{\alpha\beta} \right) \tag{38}$$

where $\omega^{\alpha} \equiv Ku^{\alpha}$, $\omega^4 \equiv K\frac{p}{\rho h}$ and $K^2 \equiv \sqrt{-g}\rho h = -g_{\alpha\beta}\omega^{\alpha}\omega^{\beta}$. The vector $\mathbf{F}^0$ represents the state vector (the unknowns) and each vector $\mathbf{F}^i$ is the corresponding flux in the coordinate direction x^i.

Eulderink and Mellema computed the appropriate "Roe matrix" [164] for vector (38) and obtained the corresponding spectral decomposition. The characteristic information is used to solve the system numerically using Roe's generalized approximate Riemann solver. Roe's linearization can be expressed in terms of the average state $\tilde{\omega} = \frac{\omega_L + \omega_R}{K_L + K_R}$, where L and R denote the left and right states in a Riemann problem (see Section 3.2). Further technical details can be found in [54, 56].

The performance of their general relativistic Roe solver was tested in a number of one-dimensional problems for which an exact solution is known including non-relativistic shock tubes, special relativistic shock tubes and spherical accretion of dust and a perfect fluid on to a (static) Schwarzschild black hole. In its special relativistic version it has been used in the study of the confinement properties of relativistic jets [55]. No astrophysical applications in strong-field general relativistic flows have yet been attempted with this formulation.

2.2.2 Papadopoulos and Font

In this formulation the spatial velocity components of the 4-velocity, u^i, together with the rest-frame density and internal energy, ρ and ε, provide a unique description of the state of the fluid and are taken as the *primitive* variables. They constitute a vector in a five dimensional space $\mathbf{w} = (\rho, u^i, \varepsilon)$. The initial value problem for equations (7) and (8) is defined in terms of another vector in the same fluid state space, namely the *conserved variables*, $\mathbf{U}$, individually denoted (D, S^i, E):

$$D = \mathbf{U}^0 = J^0 = \rho u^0 \,, \tag{39}$$

$$S^i = \mathbf{U}^i = T^{0i} = \rho h u^0 u^i + p g^{0i} \,, \tag{40}$$

$$E = \mathbf{U}^4 = T^{00} = \rho h u^0 u^0 + p g^{00} \,. \tag{41}$$

Note that these variables slightly differ from previous choices (see, e.g., Eqs. (22), (30), (31), (32) and (38)). With those definitions the equations take the standard conservation law form,

$$\frac{\partial(\sqrt{-g}\mathbf{U}^A)}{\partial x^0} + \frac{\partial(\sqrt{-g}\mathbf{F}^j)}{\partial x^j} = \mathbf{S} \,, \tag{42}$$

with $A = (0, i, 4)$. The flux vectors $\mathbf{F}^j$ and the source terms $\mathbf{S}$ (which depend only on the metric, its derivatives and the undifferentiated stress energy tensor), are given by

$$\mathbf{F}^j = (J^j, T^{ji}, T^{j0}) = (\rho u^j, \rho h u^i u^j + p g^{ij}, \rho h u^0 u^j + p g^{0j}) \tag{43}$$

$$\mathbf{S} = (0, -\sqrt{-g}\,\Gamma^i_{\mu\lambda} T^{\mu\lambda}, -\sqrt{-g}\,\Gamma^0_{\mu\lambda} T^{\mu\lambda}). \tag{44}$$

The state of the fluid is uniquely described using either vector of variables, i.e., $\mathbf{U}$ or $\mathbf{w}$, and one can be obtained from the other via the definitions (39)-(41) and the use of the normalization condition for the 4-velocity, $g_{\mu\nu}u^\mu u^\nu = -1$.

The local characteristic structure of the previous equations has been presented in [152]. The formulation has proved well suited for the numerical implementation of HRSC schemes. A comprehensive numerical study of this approach was also presented in [152] where it was applied to simulate one-dimensional relativistic flows on null spacetime foliations. The demonstrations performed include standard shock tube tests in Minkowski spacetime, perfect fluid accretion on to a Schwarzschild black hole using ingoing null Eddington-Finkelstein coordinates and dynamical spacetime evolutions of constant density and TOV stars (i.e., stellar models satisfying the Tolman-Oppenheimer-Volkoff equilibrium equations) sliced along the radial null cones and accretion of self-gravitating matter onto a central black hole.

Procedures for integrating various forms of the hydrodynamic equations on null hypersurfaces have been presented before [93] (see [22] for a recent implementation). This approach is geared towards smooth isentropic flows. A Lagrangian method, applicable in spherical symmetry, has been presented by [125]. Recent work in [50] includes a Eulerian, non-conservative, formulation for general fluids in null hypersurfaces and spherical symmetry, including their *matching* to a spacelike section.

A technical remark must be included here: In all conservative formulations reviewed in Sections 2.1.3, 2.2.1 and 2.2.2, the time-update of the numerical algorithm is applied to the conserved quantities $\mathbf{U}$. After the update the vector of primitive quantities must be reevaluated, as those are needed in the Riemann solver (see Section 3.1.2). The relation between the two sets of variables is not in closed form and, hence, the update of the primitive variables is done using a root-finding procedure, typically a Newton-Raphson algorithm. This feature may lead to accuracy loses in regions of low density and small speeds, apart from being computationally inneficient. Specific details on this issue can be found in [12, 56, 152]. We note that the covariant formulation discussed in this section, when applied to null spacetime foliations, allows for an explicit recovery of the primitive variables, as a consequence of the particular form of the Bondi-Sachs metric. We end pointing out that this formulation has been developed for a perfect fluid EOS. Extensions to account for generic EOS are currently underway.

2.3 Going further

Formulations of the equations of non-ideal hydrodynamics in General Relativity are also available in the literature. The term "non-ideal" includes here effects such as viscosity, magnetic fields and radiative transfer. These non-adiabatic effects can play a major role in some astrophysical systems as, e.g., accretion disks.

The equations of viscous hydrodynamics, the Navier-Stokes-Fourier equations, have been formulated in relativity in terms of causal dissipative relativistic fluids (see [133] for a review). These extended fluid theories are still almost unexplored, numerically, in astrophysical systems. The reason may be the lack of an appropriate formulation well-suited for numerical studies. Peitz and Appl [154] have recently provided a 3+1 coordinate-free representation of different types of dissipative relativistic fluid theories [106, 52, 94] which has the potentiality of being well adapted to numerical applications.

The inclusion of magnetic fields and the development of formulations for the magneto-hydrodynamic equations attractive to numerical studies, in General Relativity, is very limited. Numerical approaches in Special Relativity are presented in [99, 197]. 3+1 representations of relativistic magneto-hydrodynamics can be found in [185, 58]. In [214] the transport of energy and angular momentum in magneto-hydrodynamical accretion onto a rotating black hole was studied adopting Wilson's formulation for the hydrodynamic equations (conveniently modified to account for the magnetic terms) and the magnetic induction equation was solved using the constrained transport method of [58]. Recently [98] have performed the first magneto-hydrodynamical simulation, in general relativity, of magnetically driven relativistic jets from an accretion disk around a Schwarzschild black hole.

The interaction between matter and radiation fields, present in different levels of complexity in all astrophysical systems, is described by the equations of radiation hydrodynamics. The Newtonian framework is highly developed (see, e.g. [124]; the special relativistic transfer equation is also considered in that reference). General relativistic formulations of radiative transfer in curved spacetimes are considered in, e.g., [163] and [217] (see also references therein).

3 Numerical schemes

This section describes the numerical schemes, mainly those based on finite differences, specifically designed to solve non-linear hyperbolic systems of conservation laws. As discussed in the previous section, the equations of general relativistic hydrodynamics fall in this category. Although schemes based on artificial viscosity techniques are also considered the emphasis is given on the so-called high-resolution shock-capturing (HRSC) schemes (or Godunov-type methods), based on (either exact or approximate) solutions of local Riemann problems using the characteristic fields of the equations. Such finite difference schemes (or, in general, finite volume schemes) have been the subject of diverse review articles and textbooks (see, e.g., [104, 105, 90]). For this reason only the most relevant features will be covered here, referring the reader to the appropriate literature for further details. In particular, an excellent introduction on the implementation of HRSC schemes in special relativistic hydrodynamics is presented in [115]. Alternative techniques to finite differences, such as Smoothed

Particle Hydrodynamics and (pseudo) Spectral Methods are briefly considered last.

3.1 Finite difference schemes

Any system of equations presented in the previous section can be solved numerically by replacing the partial derivatives by finite differences on a discrete numerical grid and then advancing the solution in time via some time-marching algorithm. Hence, specification of $\mathbf{U}$ on an initial hypersurface, together with a suitable EOS, followed by a recovery of the primitive variables leads to the computation of the fluxes and source terms. In doing so, the first time derivative of the data is obtained, which then leads to the formal propagation of the solution forward in time, with a time-step constrained by the Courant-Friedrichs-Lewy (CFL) condition.

Examples of this type of schemes can be found in e.g. [104]. In particular, for hyperbolic systems there exists a very extensive literature. The hydrodynamic equations constitute a non-linear hyperbolic system and, hence, smooth initial data can give rise to discontinuous data (cross of characteristics in the case of shocks) in a finite time during the evolution. As a consequence classical finite difference schemes present important deficiencies when dealing with such systems. Typically, first order schemes are too dissipative across discontinuities (excessive smearing) and second order (or higher) schemes produce spurious oscillations near discontinuities which do not dissapear as the grid is refined. Standard finite difference schemes have been conveniently modified in two ways to obtain accurate representations of discontinuous solutions as we discuss next.

3.1.1 Artificial viscosity schemes

High-resolution schemes based on the idea of modifying the equations by introducing some terms providing *artificial viscosity* to damp the amplitude of spurious oscillations near discontinuities were originally proposed by von Neumann and Richtmyer [200] to solve the (classical) Euler equations. The basic idea is to introduce a purely artificial dissipative mechanism whose form and strength are such that the shock transition is smooth, extending over a small number of intervals Δx of the space variable. In this approach the equations are discretised using a high order finite difference method (e.g., a second order Lax-Wendroff scheme), which gives good results in smooth parts of the flow solution, adding an artificial viscosity term Q to the hyperbolic system which only acts there where discontinuities arise. The term Q must vanish as the grid is refined and the time step is reduced, i.e., $\Delta t, \Delta x \to 0$.

Von Neumann and Richtmyer derived the following expression for the viscosity term:

$$Q = \begin{cases} -\alpha \frac{\partial v}{\partial x} & \text{if } \frac{\partial v}{\partial x} < 0 \text{ or } \frac{\partial \rho}{\partial t} > 0 \\ 0 & \text{otherwise} \end{cases}$$

with $\alpha = \rho(k\Delta x)^2 \frac{\partial v}{\partial x}$, v being the fluid velocity, ρ the density, Δx the spatial interval and k a constant parameter whose value is conveniently adjusted in every numerical experiment. This parameter controls the number of zones in which shock waves are spread.

This type of recipe, with minor modifications, has been used in all numerical simulations employing May and White's formulation, mostly in the context of gravitational collapse, as well as Wilson's formulation. So, for example, in May and White's code [118] the artificial viscosity term, obtained in analogy with the one originally proposed by von Neumann and Richtmyer [200], is introduced in the equations accompanying the pressure, in the form:

$$Q = \begin{cases} \rho(\frac{a\Delta m}{R^2})^2 \frac{\partial R^2 u}{\partial m}/\Gamma & \text{if } \frac{\partial \rho}{\partial t} > 0 \\ 0 & \text{otherwise} \end{cases}$$

Further examples of equivalent expressions for the artificial viscosity terms, in the context of Wilson formulation, can be found in, e.g., [203, 85].

The main advantages of the artificial viscosity approach are: (i) it is straightforward to implement (compared to the HRSC schemes which need of the characteristic fields of the equations) and (ii) it is computationally very efficient. As disadvantages experience has shown that this procedure is (i) problem dependent and (ii) inaccurate for ultra relativistic flows [143]. Additionally, the artificial viscosity approach has the implicit difficulty of finding the appropriate form for Q that introduces the necessary amount of dissipation to reduce the spurious oscillations and, at the same time, avoids introducing excessive smearing in the discontinuities. In many instances both properties are difficult to achieve simultaneously. A comprehensive numerical study of artificial viscosity induced errors in strong shock calculations in Newtonian hydrodynamics (including also proposed improvements) was presented by Noh [142].

3.1.2 High-resolution shock-capturing (HRSC) schemes

Since [112] it has been gradually demonstrated ([64, 56, 165, 60, 12, 201, 159]) that conservative methods exploiting the hyperbolic character of the hydrodynamic equations are optimally suited for accurate integrations, even well inside the ultrarelativistic regime. The explicit knowledge of the characteristic fields (eigenvalues) of the equations, together with the corresponding eigenvectors, provides the mathematical (and physical) framework for such integrations, by means of either exact or approximate Riemann solvers. These solvers compute, at every interface of the numerical grid, the solution of local Riemann problems (i.e., the simplest initial value problem with discontinuous initial data). Hence, a HRSC scheme automatically guarantees that the physical discontinuities appearing in the solution, e.g., shock waves, will be treated consistently (the *shock-capturing* property). HRSC schemes also produce stable and sharp discrete shock profiles, while providing a high order of accuracy, typically second order or more, in smooth parts of the solution.

To focus the discussion let us consider the system as formulated in Eq. (34). Let us consider a single computational cell of our discrete spacetime. Let Ω be a region (simply connected) of the four-dimensional manifold $\mathcal{M}$, bounded by a closed three-dimensional surface $\partial\Omega$. We take the 3-surface $\partial\Omega$ as the standard-oriented hyper-parallelepiped made up of two spacelike surfaces $\{\Sigma_{x^0}, \Sigma_{x^0+\Delta x^0}\}$ plus timelike surfaces $\{\Sigma_{x^i}, \Sigma_{x^i+\Delta x^i}\}$ that join the two temporal slices together. By integrating system (34) over a domain Ω of a given spacetime, the variation in time of the state vector $\mathbf{U}$ within Ω is given – keeping apart the source terms – by the fluxes $\mathbf{F}^i$ through the boundary $\partial\Omega$. The integral form of system (34) is

$$\int_\Omega \frac{1}{\sqrt{-g}} \frac{\partial \sqrt{\gamma}\mathbf{U}}{\partial x^0} d\Omega + \int_\Omega \frac{1}{\sqrt{-g}} \frac{\partial \sqrt{-g}\mathbf{F}^i}{\partial x^i} d\Omega = \int_\Omega \mathbf{S} d\Omega \tag{45}$$

which can be written in the following conservation form, well-adapted to numerical applications:

$$\begin{aligned}
& (\overline{\mathbf{U}}\Delta V)_{x^0+\Delta x^0} - (\overline{\mathbf{U}}\Delta V)_{x^0} = \\
- & \left(\int_{\Sigma_{x^1+\Delta x^1}} \sqrt{-g}\hat{\mathbf{F}}^1 dx^0 dx^2 dx^3 - \int_{\Sigma_{x^1}} \sqrt{-g}\hat{\mathbf{F}}^1 dx^0 dx^2 dx^3 \right) \\
- & \left(\int_{\Sigma_{x^2+\Delta x^2}} \sqrt{-g}\hat{\mathbf{F}}^2 dx^0 dx^1 dx^3 - \int_{\Sigma_{x^2}} \sqrt{-g}\hat{\mathbf{F}}^2 dx^0 dx^1 dx^3 \right) \\
- & \left(\int_{\Sigma_{x^3+\Delta x^3}} \sqrt{-g}\hat{\mathbf{F}}^3 dx^0 dx^1 dx^2 - \int_{\Sigma_{x^3}} \sqrt{-g}\hat{\mathbf{F}}^3 dx^0 dx^1 dx^2 \right) \\
+ & \int_\Omega \mathbf{S} d\Omega
\end{aligned} \tag{46}$$

where

$$\overline{\mathbf{U}} = \frac{1}{\Delta V} \int_{\Delta V} \sqrt{\gamma}\mathbf{U} dx^1 dx^2 dx^3, \tag{47}$$

$$\Delta V = \int_{x^1}^{x^1+\Delta x^1} \int_{x^2}^{x^2+\Delta x^2} \int_{x^3}^{x^3+\Delta x^3} \sqrt{\gamma} dx^1 dx^2 dx^3. \tag{48}$$

An important property of writing a numerical scheme in conservation form is that, in the absence of sources, the (physically) conserved quantities, according to the partial differential equations, are numerically conserved by the finite difference equations.

The "hat" symbol appearing on the fluxes of Eq. (46) indicates the numerical fluxes. These are recognized as approximations to the time-averaged fluxes across the cell-interfaces, which depend on the solution at those interfaces, $\mathbf{U}(x^i + \Delta x^i/2, x^0)$, during a time step. At the cell-interfaces the flow conditions can be discontinuous and, following the seminal idea of Godunov [74], the numerical fluxes can be obtained by solving a collection of local Riemann problems.

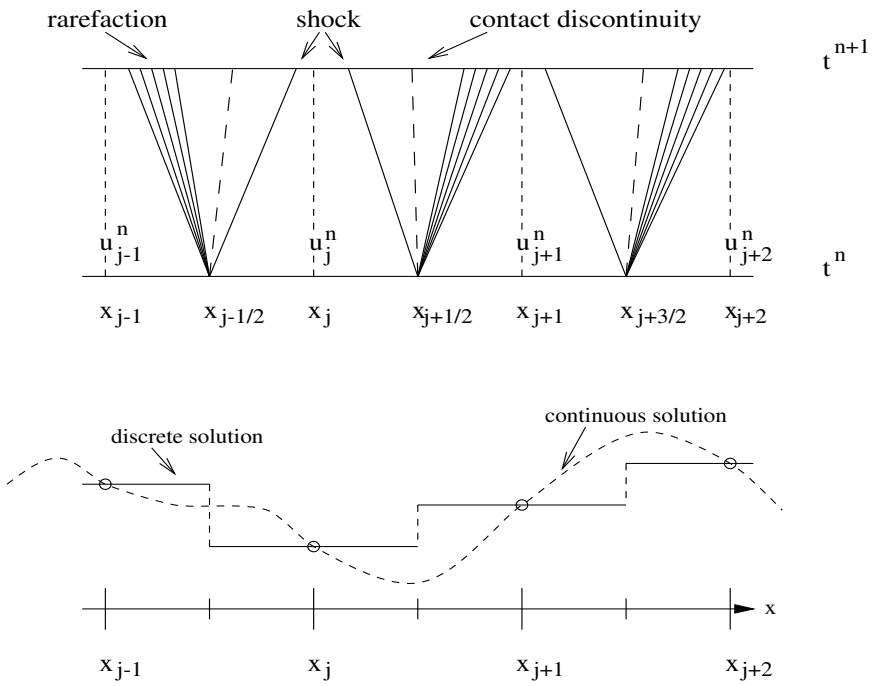

Figure 2: Godunov's scheme: local solutions of Riemann problems. At every interface, $x_{j-\frac{1}{2}}$, $x_{j+\frac{1}{2}}$ and $x_{j+\frac{3}{2}}$, a local Riemann problem is set up as a result of the discretization process (bottom panel). At time t^n these discontinuities decay into three elementary waves which propagate the solution forward to the next time level t^{n+1} (top panel). The time step of the numerical scheme must satisfy the Courant-Friedrichs-Lewy condition, being small enough to prevent the waves from advancing more than $\Delta x/2$ in Δt.

This is depicted in Fig. 2. The continuous solution is locally averaged on the numerical grid, a process which leads to the appearance of discontinuities at the cell-interfaces. Every discontinuity decays into three elementary waves: a shock wave, a rarefaction wave and a contact discontinuity. The complete structure of the Riemann problem can be solved analytically (see [74] for the solution in Newtonian hydrodynamics and [113] in special relativistic hydrodynamics) and, accordingly, used to update the solution forward in time.

For reasons of efficiency and, particularly, in multidimensions, the exact solution of the Riemann problem is frequently avoided and linearized (approximate) Riemann solvers are preferred. These solvers are based in the exact solution of Riemann problems corresponding to a linearized version of the original system of equations and, after extensive experimentation, they are found to produce results comparable to those obtained with the exact solver (see [115] for a sum-

mary of such approximate solvers in special relativistic hydrodynamics).

In the frame of the local characteristic approach the numerical fluxes are computed according to some generic flux-formula which makes use of the characteristic information of the system. For example, in Roe's approximate Riemann solver it adopts the following functional form:

$$\hat{\mathbf{F}}^i = \frac{1}{2}\left(\mathbf{F}^i(\mathbf{w}_{\rm R}) + \mathbf{F}^i(\mathbf{w}_{\rm L}) - \sum_{n=1}^{5} |\widetilde{\lambda}_n| \Delta\widetilde{\omega}_n \widetilde{\mathbf{r}}_n \right) \tag{49}$$

where $\mathbf{w}_{\rm L}$ and $\mathbf{w}_{\rm R}$ represent the values of the primitive variables at the left and right sides, respectively, of the corresponding interface. They are obtained from the cell-centered quantities after a suitable monotone reconstruction procedure. The way these variables are computed determines the spatial order of the numerical algorithm and controls the local jumps at every interface. If these jumps are monotonically reduced the scheme provides more accurate initial guesses for the solution of the local Riemann problems. A wide variety of cell reconstruction procedures is available in the literature. Among the most popular slope limiter procedures for Total-Variation-Diminishing (TVD) schemes [78] are the second order, piecewise linear reconstruction, introduced by van Leer [196] in the design of the MUSCL scheme (Monotonic Upstream Scheme for Conservation Laws) and the third order, piecewise parabolic reconstruction developed by Colella and Woodward [44] in their Piecewise Parabolic Method (PPM). High order piecewise polynomial functions are also available for Essentially Non-Oscillatory (ENO) schemes [79].

The last term in the flux-formula represents the numerical viscosity of the scheme and it makes explicit use of the characteristic information of the Jacobian matrices of the system. This information is used to provide the appropriate amount of numerical dissipation to obtain accurate representations of discontinuous solutions without excessive smearing avoiding, at the same time, the growth of spurious numerical oscillations associated to the Gibbs phenomenon. Hence, $\{\widetilde{\lambda}_n, \widetilde{\mathbf{r}}_n\}_{n=1\ldots5}$ are, respectively, the eigenvalues and right-eigenvectors of the Jacobian matrix and quantities $\{\Delta\widetilde{\omega}_n\}_{n=1\ldots5}$ are the jumps of the characteristic variables across each characteristic field. They are obtained by projecting the jumps of the state-vector variables with the left-eigenvectors matrix:

$$\mathbf{U}(\mathbf{w}_{\rm R}) - \mathbf{U}(\mathbf{w}_{\rm L}) = \sum_{n=1}^{5} \Delta\widetilde{\omega}_n \widetilde{\mathbf{r}}_n \tag{50}$$

The "tilde" indicates that the corresponding fields are averaged at the cell interfaces from the left and right (reconstructed) values.

During the last few years most of the *classical* Riemann solvers developed in fluid dynamics have been extended to Relativity: Eulderink [56], as discussed in Section 2.2.1, has explicitly derived a relativistic Roe Riemann solver [164], Schneider et al. [171] carried out the extension of Einfeldt's HLLE method [80,

53], Martí and Müller [114] extended the PPM method of Woodward and Colella [210], Wen et al [201] extended Glimm's method, Dolezal and Wong [47] put into practice Shu-Osher ENO techniques, Balsara [11] extended Colella's two-shock approximation and Donat et al. [48] extended Marquina's method [49]. The interested reader is referred to [115] for a comprehensive description of such solvers in special relativistic hydrodynamics.

3.2 Other techniques

Two of the most frequently employed alternatives to finite difference schemes are Smoothed Particle Hydrodynamics (SPH) and (pseudo) Spectral Methods.

3.2.1 Smoothed particle hydrodynamics

The Lagrangian particle method SPH, derived independently by Lucy [107] and Gingold and Monaghan [71], has shown successful performance to model fluid flows in astrophysics and cosmology. Most studies to date consider Newtonian flows and gravity, enhanced with the inclusion of the fluid self-gravity. Reviews of the classical SPH equations are abundant in the literature (see, e.g., [130, 132] and references therein). The reader is addressed to [132] for a summary of comparisons between SPH and HRSC methods.

Recently, implementations of SPH to handle (special) relativistic (and even ultra relativistic) flows have been developed (see, e.g., [43] and references therein). However, SPH has been scarcely applied to simulate relativistic flows in curved spacetimes. Relevant references include [96, 101, 102, 184].

Following [101] let us describe the implementation of an SPH scheme in general relativity. Given a function $f(\mathbf{x})$, its mean *smoothed* value $\langle f(\mathbf{x})\rangle$, ($\mathbf{x} = (x, y, z)$) can be obtained from

$$\langle f(\mathbf{x})\rangle \equiv \int W(\mathbf{x}, \mathbf{x}'; h) f(\mathbf{x}') \sqrt{g'} d^3x' \tag{51}$$

where W is the kernel, h the smoothing length and $\sqrt{g'}d^3x'$ the volume element. The kernel is required to satisfy a normalization condition

$$\int W(\mathbf{x}, \mathbf{x}'; h) \sqrt{g'} d^3x' = 1 \tag{52}$$

which is assured by choosing $W(\mathbf{x}, \mathbf{x}'; h) = \xi(\mathbf{x})\Omega(v)$, with $v = |\mathbf{x} - \mathbf{x}'|/h$, $\xi(\mathbf{x})$ a normalization function and $\Omega(v)$ a standard spherical kernel.

The smooth approximation of gradients of scalar functions can be written

$$\langle \nabla f(\mathbf{x})\rangle = \nabla \langle f(\mathbf{x})\rangle - \langle f(\mathbf{x})\rangle \nabla \ln \xi(\mathbf{x}) \tag{53}$$

and the corresponding to the divergence of a vector reads

$$\langle \nabla \cdot \mathbf{A}(\mathbf{x})\rangle = \nabla \cdot \langle \mathbf{A}(\mathbf{x})\rangle - \langle \mathbf{A}(\mathbf{x})\rangle \cdot \ln \xi(\mathbf{x}). \tag{54}$$

Discrete representations of these procedures are obtained after introducing the number density distribution of particles $\langle n(\mathbf{x})\rangle \equiv \sum_{a=1}^{N} \delta(\mathbf{x}-\mathbf{x}_a)/\sqrt{g}$, with $\{\mathbf{x}_a\}_{a=1,\ldots,N}$ the collection of N-particles where the functions are known. The previous representations read then:

$$\langle f(\mathbf{x}_a)\rangle = \xi(\mathbf{x}_a)\sum_{b=1}^{N}\frac{f(\mathbf{x}_b)}{\langle n(\mathbf{x}_b)\rangle}\Omega_{ab}, \tag{55}$$

$$\langle \nabla f(\mathbf{x}_a)\rangle = \xi(\mathbf{x}_a)\sum_{b=1}^{N}\frac{f(\mathbf{x}_b)}{\langle n(\mathbf{x}_b)\rangle}\nabla_{\mathbf{x}_a}\Omega_{ab}, \tag{56}$$

$$\langle \nabla\cdot\mathbf{A}(\mathbf{x}_a)\rangle = \xi(\mathbf{x}_a)\sum_{b=1}^{N}\frac{\mathbf{A}(\mathbf{x}_b)}{\langle n(\mathbf{x}_b)\rangle}\cdot\nabla_{\mathbf{x}_a}\Omega_{ab}, \tag{57}$$

with $\Omega_{ab} \equiv \Omega(\mathbf{x}_a, \mathbf{x}_b; h)$. These approximations can be used to derive the SPH version of the general relativistic hydrodynamic equations. Explicit formulae are reported in [101]. The time evolution of the final system of ODEs is performed in [101] using a second-order Runge-Kutta time integrator with adaptive time step. As in non Riemann solver based finite volume schemes, in SPH simulations involving the presence of shock waves, artificial viscosity terms must be introduced as a viscous pressure term [108].

Recently, [184] have developed a Lagrangian conservation form of the general relativistic hydrodynamic equations for perfect fluids, with artificial viscosity, in arbitrary background spacetimes. Within that formulation [184] have built a general relativistic SPH code using the *standard* SPH formalism as known from Newtonian fluid dynamics (in contrast to previous approaches [108, 96, 101]). The conservative character of their scheme allows to model ultra relativistic flows including shocks with Lorentz factors as large as 1000.

3.2.2 Spectral methods

The basic principle underlying spectral methods consists on transforming the partial differential equations into a system of ordinary differential equations by means of expanding the solution into a series on a complete basis. The mathematical theory of these schemes is presented in [76, 38]. Spectral methods are particularly well suited to solve elliptic and parabolic equations. Good results can also be obtained for hyperbolic equations as long as no discontinuities appear in the solution. When a discontinuity is present some amount of artificial viscosity must be added to obtain a smooth solution. In the specific case of relativistic problems, where coupled systems of elliptic equations (i.e., the Einstein constraint equations) and hyperbolic equations (i.e., hydrodynamics) must be solved, an interesting solution strategy is to use spectral methods for the elliptic equations and HRSC schemes for the hyperbolic ones. Using such combined methods first results have been obtained in one-dimensional supernova collapse in the framework of a tensor-scalar theory of gravitation [144].

Following [28] we illustrate the main ideas of spectral methods considering the quasi-linear one-dimensional scalar equation:

$$\frac{\partial u}{\partial t} = \frac{\partial^2 u}{\partial x^2} + \lambda u \frac{\partial u}{\partial x}, \qquad t \geq 0, \qquad x \in [0,1], \tag{58}$$

with $u = u(t,x)$ and λ a constant parameter. In the linear case ($\lambda = 0$), and assuming the function u to be periodic, spectral methods expand the function in a Fourier series:

$$u(x,t) = \sum_{k=0}^{\infty} [a_k(t)\cos(2\pi k x) + b_k(t)\sin(2\pi k x)]. \tag{59}$$

From the numerical point of view, the series is truncated for a suitable value of k. Hence, Eq. (58), with $\lambda = 0$, can be rewritten as

$$\frac{da_k}{dt} = -k^2 a_k(t), \qquad \frac{db_k}{dt} = -k^2 b_k(t). \tag{60}$$

Finding a solution of the original equation is then equivalent to solve an "infinite" system of ordinary differential equations, where the initial values of coefficients a_k and b_k are given by the Fourier expansion of $u(x,0)$.

In the non-linear case, $\lambda \neq 0$, spectral methods, or, in this case, more correctly pseudo-spectral methods, proceed in a more intrincated way: first, the derivative of u is computed in the Fourier space, then, they come back to the configuration space by an inverse Fourier transform, multiply $\partial u/\partial x$ by u in the configuration space and, finally, come back again to the Fourier space.

The particular set of trigonometric functions used for the expansion is chosen because it fulfills automatically the boundary conditions and because a fast transform algorithm is available. If the initial or boundary conditions are not periodic, Fourier expansion is no longer useful because of the presence of a Gibbs phenomenon at the boundaries of the interval. Legendre or Chebyshev polynomials are in this case the most common base of functions used in the expansions (see [76, 38] for a discussion on the different expansions).

A comprehensive summary of applications of (pseudo) spectral methods in general relativistic astrophysics is presented in [28]. Among those involving time-dependent hydrodynamical simulations we mention the spherically symmetric collapse computations of Gourgoulhon [77] as well as the three-dimensional Newtonian simulations of [29, 109].

4 Simulations of astrophysical phenomena

We turn now to present an overview of strong-field simulations in relativistic astrophysics using the numerical methods discussed in the previous section.

With the exception of the vacuum two-body problem (i.e., the coalescence of two black holes), all realistic astrophysical systems and sources of gravitational radiation involve matter. Not surprisingly, the joint integration of the equations of motion for matter and geometry was, hence, in the minds of theorists from the very beginning of numerical relativity.

Nowadays there is a large body of numerical investigations in the literature dealing with hydrodynamical integrations in *static* background spacetimes. Most of those are based on the Wilson formulation of the hydrodynamic equations and use schemes based on finite differences with some amount of artificial viscosity. The use of conservative formulations of the equations and their characteristic information in the design of numerical schemes has started in more recent years.

On the other hand, time-dependent simulations of self-gravitating flows in general relativity, evolving the spacetime *dynamically* with the Einstein equations coupled to a hydrodynamic source, constitute a much smaller sample. Although there is much recent interest in this direction, only the spherically symmetric case (1D) has been extensively studied and, to some extent, can be considered essentially solved. In axisymmetry, i.e. 2D, fewer attempts have been made, with most of them devoted to the study of the gravitational collapse and bounce of rotating stellar cores and the subsequent emission of gravitational radiation. Three-dimensional simulations have only started more recently. The effort is nowadays mainly focused in the study of the coalescence and merging of compact neutron star binaries (as well as the vacuum black hole binary counterpart). These theoretical investigations are driven by the emerging possibility of detecting gravitational waves in a few years time with different experimental efforts currently underway.

In the following we review the status of the numerical investigations in three astrophysical scenarios all involving strong gravitational fields and, hence, relativistic physics: gravitational collapse, accretion on to black holes and hydrodynamical evolution of binary neutron stars. Relativistic cosmology, another area where fundamental advances have been accomplished through numerical simulations, is not considered. The interested reader is addressed to the review by Anninos [6] and to the research papers [39, 40, 7].

4.1 Gravitational collapse

The study of gravitational collapse of massive stars has been largely pursued numerically over the years. This problem was already the main motivation when May and White built the first one-dimensional code [118, 119]. It is worth to notice that this code was conceived to integrate the coupled system of Einstein field equations and relativistic hydrodynamics, sidestepping Newtonian approaches.

By browsing through the literature one immediately realizes that the numerical study of gravitational collapse was neatly splitted into two main directions

since the early investigations. First, the numerical *astrophysical community* has traditionally focused on the physics of the (type II) Supernova mechanism, i.e., collapse of unstable iron cores followed by a bounce and explosion. Nowadays, numerical simulations are highly developed, as they include rotation and detailed state-of-the-art microphysics (e.g., EOS and sophisticated treatments for neutrino transport). These studies are currently performed, routinely, using 3D Cartesian grids with advanced HRSC schemes. Progress in this direction has been achieved, however, at the expense of necessary approximations in the treatment of the hydrodynamics and gravitational field, by using Newtonian physics. In this approach the emission of gravitational radiation is computed through the quadrupole formula. For a recent review of the current status in this direction see [132] and references therein.

On the other hand, the *numerical relativity community* has been more interested, since the beginning, in highlighting those aspects of the collapse problem having to do with relativistic gravity, in particular the emission of gravitational radiation from a non-spherical collapse. Much of the effort has focused on developing reliable numerical schemes to evolve the gravitational field and much less emphasis, if any, has been given to the details of the microphysics of core collapse. This approach has also considered gravitational collapse leading to black hole formation, employing relativistic hydrodynamics and gravity. Quite surprisingly both approaches have barely interacted over the years, except for a handful of simulations in spherical symmetry. We turn next to their description.

4.1.1 One dimensional simulations

The standard model of type II Supernovae involves the presence of a strong shock wave formed at the edge between the homologous inner core and the outer core which falls at roughly free-fall speed. An schematic illustration of the dynamics of this system is depicted in Fig. 3. The shock is produced after the bounce of the inner core when its density exceeds nuclear density. Numerical simulations have tried to elucidate if this shock would be strong enough to propagate outwards through the star's mantle and envelope given certain initial conditions for the material in the core, an issue subjected to important uncertainties in the nuclear EOS, as well as in the outer layers of the star. In the accepted scenario which has emerged from the numerical simulations, the existence of the shock wave together with neutrino re-heating that re-energizes it (in the so-called delayed-mechanism by which the stalled prompt supernova shock is reactivated by an increase in the pressure behind it due to neutrino energy deposition [205, 21]) and convective overturn which rapidly transports energy into the shocked region [45, 20] (and which can lead to large-scale deviations from spherically symmetric explosions), are necessary for all plausible explosion mechanisms.

The path to reach such conclusions has been delineated from numerical simulations in one spatial dimension. Fully relativistic simulations of microphysically

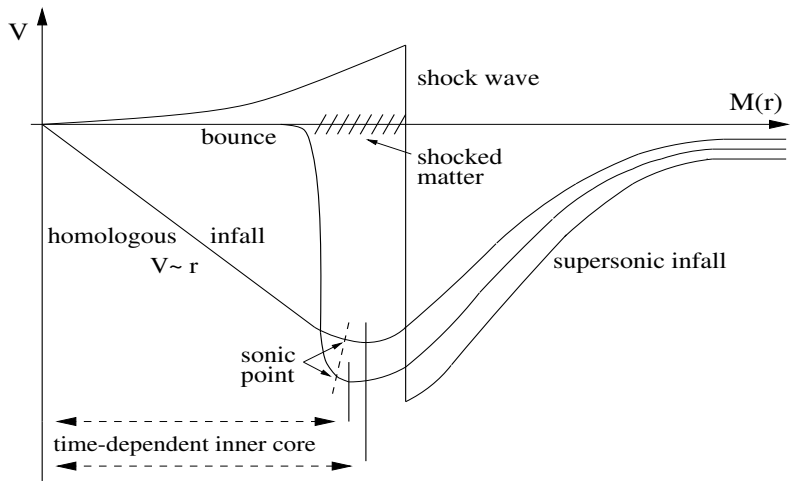

Figure 3: Schematic profiles of the velocity versus radius at three different times during core collapse: at the point of "last good homology", at bounce and at the time when the shock wave has just detached from the inner core.

detailed core collapse off spherical symmetry are still absent and they could introduce some modifications. The overall picture just described above has been demonstrated in multidimensions using sophisticated Newtonian models as is extensively documented in [132].

May and White's formulation and their corresponding one-dimensional code formed the basis of the majority of subsequent spherically symmetric codes to study the collapse problem. Wilson [202] investigated the effect of neutrino transport on the stellar collapse concluding that heat conduction by neutrinos does not produce the ejection of material, in contrast to previous results [46, 8]. The code solved the coupled set of hydrodynamic and Einstein equations, supplemented with a Boltzmann transport equation to describe the neutrino flow. Van Riper [198] used a spherically symmetric general relativistic code to study adiabatic collapse of stellar cores, considering the purely hydrodynamical bounce as the preferred explosion mechanism. The important role of general relativistic effects to produce collapses otherwise absent in Newtonian simulations was emphasized. Bruenn [35] developed a code in which the neutrino transport was handled with an approximation, the multigroup flux-limited diffusion. Baron et al [15] obtained a successful and very energetic explosion for a model with a particular small value of the incompressibility modulus of symmetric nuclear matter at zero temperature, $K_0^{sym} = 180 MeV$ (whose precise value, nowadays preferred around $240 MeV$ [73], is still a matter of debate). Mayle et al [120] computed neutrino spectra from stellar collapse to stable neutron stars for different collapse models using, as [35], multigroup flux-limited diffusion for the neutrino

transport. Van Riper [199] and Bruenn [36] verified that softer supranuclear EOS, combined with general relativistic hydrodynamics, increases the chances for a prompt explosion. In [170, 169] and [122] the neutrino transport was first handled without approximation by using a general relativistic Boltzmann equation. Whereas in [170, 169] the neutrino transport is described by moments of the general relativistic Boltzmann equation in polar slicing coordinates [13], [122] used maximal slicing coordinates. Miralles et al [127], employing a realistic EOS based upon a Hartree-Fock approximation for Skyrme-type nuclear forces for densities above nuclear density, obtained results qualitatively similar to those of Baron et al [15], who used a phenomenological EOS, i.e., the explosion was favoured by soft EOS. Swesty et al [191] also focused on the role of the nuclear EOS in stellar collapse on prompt timescales. Contrary to previous results they found that the dynamics of the shock is almost independent of the nuclear incompressibility once the EOS is not unphysically softened as in earlier simulations (e.g. [198, 15, 199, 36, 127]). Swesty and coworkers used a finite temperature compressible liquid drop EOS [103]. For the shock to propagate promptly to large radius they found that the EOS must be very soft at densities just above nuclear densities, which is inconsistent with the $1.44 M_{\odot}$ neutron star mass constraint imposed by observations of the binary pulsar PSR 1913+16.

All the aforementioned investigations used artificial viscosity techniques to handle shock waves. Together with a detailed description of the microphysics, the correct numerical modeling of the shock is the major issue in stellar collapse. In this context, the use of HRSC schemes, specifically designed to capture discontinuities, is much more recent. It started in the late eighties with the Newtonian simulations performed by Fryxell et al [70] using an Eulerian second order PPM scheme (see [132] for a review of the present status). There are only a few relativistic simulations, so far restricted to spherical symmetry. Most of them have been performed by the Valencia group, first employing Newtonian gravity [111], and later relativistic gravity [91, 25, 88, 165].

Martí et al [111] implemented Glaister's approximate Riemann solver [72] into a Lagrangian Newtonian hydrodynamical code. They performed a comparison of the energetics of a stellar collapse simulation using this HRSC scheme and a standard May and White code with artificial viscosity, for the same initial model, grid size and EOS. They found that the simulation employing a Godunov-type scheme produced larger kinetic energies than the corresponding to the artificial viscosity scheme, with a factor of two difference in the maximum of the infalling velocity. Motivated by this important difference Janka et al [95] repeated this computation with a different EOS using a PPM second order Godunov-type scheme disagreeing with Martí et al [111]. The state-of-the-art implementation of the tensorial artificial viscosity terms in [95] together with the very fine numerical grids employed (unrealistic for three dimensional simulations) could be the reason of the discrepancies.

As mentioned in Section 2.2 Godunov-type methods were first used to solve the equations of general relativistic hydrodynamics in [112], where the character-

istic fields of the one-dimensional (spherically symmetric) system were derived. The first astrophysical application was stellar collapse. In [25] the hydrodynamic equations were coupled to the Einstein equations in spherical symmetry. The field equations were formulated as a first-order flux-conservative hyperbolic system for a harmonic gauge [26], somehow "resembling" the hydrodynamic equations. HRSC schemes could be applied, hence, to both systems simultaneously (only coupled through the source terms of the equations). Results for simple models of adiabatic collapse following this approach can be found in [110, 25, 88].

A comprehensive study of adiabatic, one-dimensional, core collapse using explicit HRSC schemes was presented in [165] (a similar computation using implicit schemes was later performed by [213]). In this investigation the equations for the hydrodynamics and the geometry are written using radial gauge polar slicing (Schwarzschild-type) coordinates. The collapse is modeled with an ideal gas EOS with a non-constant adiabatic index, which varies with the density as $\Gamma = \Gamma_{min} + \eta(\log\rho - \log\rho_b)$, where ρ_b is the bounce density and $\eta = 0$ if $\rho < \rho_b$ and $\eta > 0$ otherwise [198]. A set of animations of the simulations presented in [165] are included in the MPEG movies 1.1 to 1.4. They correspond to the rather stiff Model B of [165]: $\Gamma_{min} = 1.33, \eta = 5$ and $\rho_b = 2.5 \times 10^{15} g\, cm^{-3}$. The initial model is a white dwarf having a gravitational mass of $1.3862 M_\odot$. The animations show the time evolution of the radial profiles of the following fields: velocity (MPEG 1.1), logarithm of the rest-mass density (MPEG 1.2), gravitational mass (MPEG 1.3) and the square of the lapse function (MPEG 1.4).

The movies show that the shock is sharply resolved and free of spurious oscillations. The radius of the inner core at the time of maximum compression, at which the infall velocity is maximum ($v = -0.62c$), is $6.3km$. The gravitational mass of the inner core at the time of maximum compression is $\approx 1.0 M_\odot$. The minimum value quantity α^2 reaches is 0.14 which indicates the highly relativistic character of these simulations (at the surface of a typical neutron star $\alpha^2 \approx 0.75$).

Studies of black hole formation in strong field hydrodynamical simulations of gravitational collapse are less frequent [198, 175, 18, 140]. In [198], using the (Lagrangian) May and White code described previously, the mass division between neutron star and black hole formation was considered by means of general relativistic simulations. For the typical (cold) EOS used the critical state was found to lie between the collapses of $1.95 M_\odot$ and $1.96 M_\odot$ cores.

In [175] a one-dimensional code based on Wilson's hydrodynamical formulation was used to simulate a general relativistic (adiabatic) collapse to a black hole. The fluid equations were finite differenced in a mixed Eulerian-Lagrangian form with the introduction of an arbitrary "grid velocity" to ensure sufficient resolution throughout the collapse. The Einstein equations were formulated following the ADM equations. Isotropic coordinates and a maximal time slicing condition were used to avoid the physical singularity once the black hole forms.

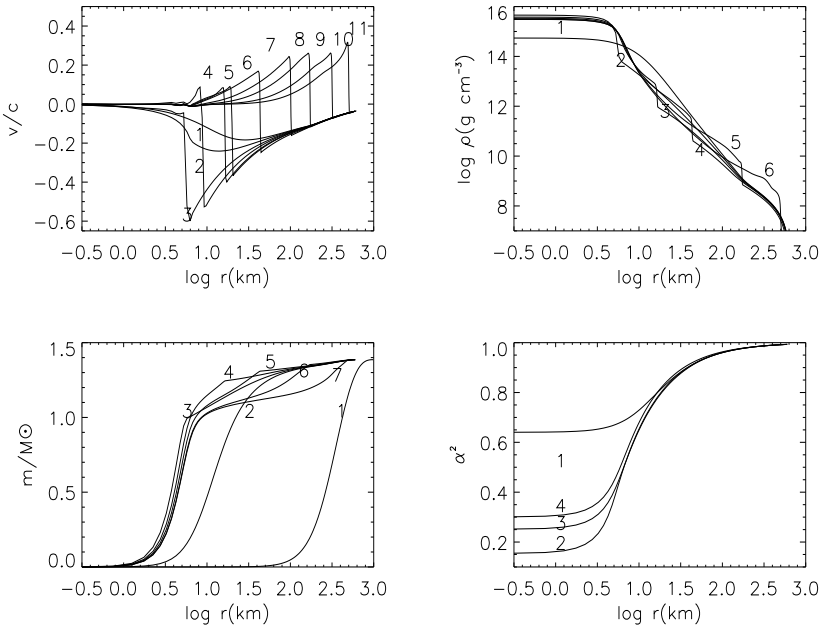

Figure 4: Animations of a relativistic adiabatic core collapse using HRSC schemes (*only snapshots of the radial profiles of various variables are shown in this plot*). The simulations are taken from Ref. [165]: (MPEG 1.1, top-left) velocity, (MPEG 1.2, top-right) logarithm of the rest-mass density, (MPEG 1.3, bottom-left) gravitational mass and (MPEG 1.4, bottom-right) lapse function squared. See text for details of the initial model.

Due to the non-dynamical character of the gravitational field in the case of spherical symmetry (i.e., the metric variables can be computed at every time step solving elliptic equations) this code was able to follow relativistic configurations for many collapse time scales $\Delta t \gg GM/c^3$ after the initial appearance of an event horizon.

A Lagrangian scheme based on the Misner and Sharp [128] formulation for spherically symmetric gravitational collapse (as in [198]) was developed by [18]. The novelty of this code was the use of an outgoing null coordinate u (as suggested previously by [86]) instead of the usual Schwarzshild time t appearing in the Misner and Sharp equations. These coordinates are ideally suited to study black hole formation as they never cross the black hole event horizon. The code solved the Hernández-Misner equations [86] (or, alternatively, the Misner-Sharp equations) by an explicit finite difference scheme similar to [198]. In [18] the collapse of a $1.4M_\odot$ polytrope with $\Gamma = 4/3$ to a black hole was compared

to [198], using the Misner-Sharp equations, finding a 10% agreement. However, the evolution stopped after the formation of the apparent horizon. This work demonstrated numerically that the use of a retarded time coordinate allowed for much longer evolutions after black hole formation. The Lagrangian character of this code has prevented its multidimensional extension.

Recently [140] have studied critical collapse of a spherically symmetric perfect fluid with EOS $p = (\Gamma - 1)\rho$ using a conservative form of the hydrodynamic equations and HRSC schemes[1]. The Einstein equations coupled to the hydrodynamic equations were integrated in spherical symmetry adopting the ADM formalism. The use of a conservative formulation and numerical schemes well adapted to describe ultrarelativistic flows [141] made possible to find evidence of the existence of critical solutions for large values of the adiabatic index Γ ($1.89 \leq \Gamma \leq 2$), extending the previous upper limit.

One-dimensional numerical simulations of self-gravitating matter accreting on to a black hole, formed after the gravitational collapse of a massive star, have been performed in [152]. Using the formulation outlined in Section 2.2.2 and HRSC schemes [152] performed the simulations adopting an ingoing null foliation of a spherically symmetric black hole spacetime. Such foliation has the interesting property of penetrating inside the black hole horizon, allowing for an unambiguous numerical treatment of the inner boundary. The simulations reported in [152] describe the capture of an initial Gaussian shell distribution of perfect fluid matter by a non-rotating black hole. The results show that the accretion process initiates, as expected, a rapid increase of the mass of the apparent horizon. This is depicted in Fig. 5. The horizon almost doubles its size during the first $10M - 15M$ (this is enlarged in the insert of Fig. 5). Once the main accretion process has finished, the mass of the horizon slowly increases, in a quasi-steady manner, whose rate depends on the mass accretion rate imposed at the world-tube of the integration domain.

4.1.2 Multidimensional studies

The use of general relativistic axisymmetric codes in numerical astrophysics has been largely devoted to the study of the gravitational collapse and bounce of a rotating stellar core and the subsequent emission of gravitational radiation. These studies of axisymmetric scenarios started in the early eighties when the available computer resources were still inadequate to attempt three dimensional simulations. The collapse scenario was by then the main motivation for code builders in numerical relativity, as it was considered one of the most important gravitational wave sources, in the same way that the coalescence and merging of neutron star (and/or black hole) binaries is driving the development of fully

[1]Critical phenomena in gravitational collapse were first discovered numerically in simulations of the massless Klein-Gordon field minimally coupled to gravity [42]. Since then critical phenomena arising at the threshold of black hole formation, in *parametrized* families of collapse, have been found in a variety of physical systems, including the perfect fluid model.

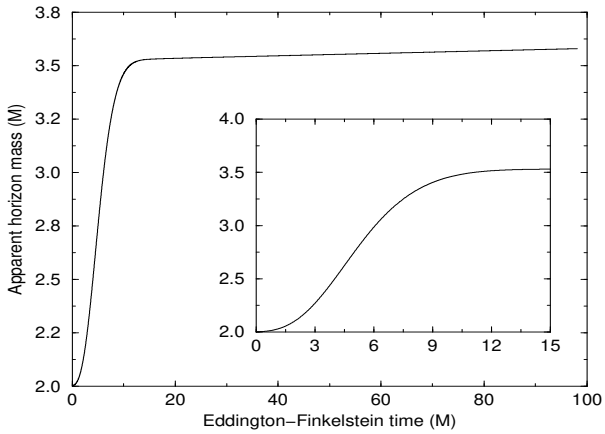

Figure 5: Evolution of the black hole apparent horizon mass during the spherical accretion of a self-gravitating perfect fluid whose density is parametrized according to $\rho = \rho_b + \rho_m \exp(-\sigma(r - r_c)^2)$ with $\rho_m = 10^{-4}$, $\sigma = 0.1$ and $r_c = 6M$. The background density ρ_b is given by the spherical Michel solution [123]. The grid extends from $r_{min} = 1.1M$ to $r_{max} = 20M$. The mass of the apparent horizon shows a rapid increase in the first $15M$ (enlarged in the insert), in coincidence with the most dynamical accretion phase. The slow, quasi-steady growth at later times is the quiet response of the black hole to the low mass accretion rate imposed at the world tube.

three dimensional codes in the nineties (and possibly will continue during the forthcoming years) in correlation with the increasing availability of computer power.

All numerical studies of axisymmetric gravitational collapse in general relativity, which will be briefly discussed next, have used Wilson's formulation of the hydrodynamic equations and finite difference schemes with artificial viscosity. The problem has not yet been considered in two (and three) dimensions using conservative formulations and HRSC schemes.

The investigations of the collapse problem started with the work of Nakamura [134], who was the first to calculate a general relativistic rotating stellar collapse. He adopted the (2+1)+1 formulation of the Einstein equations in cylindrical coordinates and introduced regularity conditions to avoid divergence behavior at coordinate singularities (the plane $Z = 0$) [135]. The equations were finite differenced using the donor cell scheme plus Friedrichs-Lax type viscosity terms. Nakamura used a "hypergeometric" slicing condition (which reduces to maximal slicing in spherical symmetry) which prevents the grid points from

hitting the singularity if a black hole forms. The simulations could track the evolution of the collapsing (perfect fluid) matter and the formation of a black hole. However, the scheme was not accurate enough to compute the emitted gravitational radiation. The reason is that the energy emitted in this process as gravitational radiation is very small compared to the total rest mass energy, making its accurate numerical computation very challenging.

Bardeen, Stark and Piran, in a series of papers [13, 188, 158, 189], revisited this problem studying the collapse of rotating relativistic polytropic stars to black holes, succeeding in computing the gravitational radiation emission. The field and hydrodynamic equations were formulated using the 3+1 formalism, with radial gauge and a mixture of (singularity avoiding) polar and maximal slicing. Their numerical results showed that the gravitational wave emission from axisymmetric rotating collapse to a black hole was very low, $\Delta E/Mc^2 < 7 \times 10^{-4}$ and that the general waveform shape was nearly independent of the details of the collapse[2]. Their parameter space survey also showed how black hole formation (of the Kerr class) occurs only for angular momenta less than a critical value.

Evans [57], building on previous work by Dykema [51], also studied the gravitational collapse problem for non-rotating matter configurations. His numerical scheme to integrate the matter fields was more sophisticated than in the previous approaches as it included monotonic upwind reconstruction procedures and flux limiters. Discontinuities appearing in the flow solutions were stabilized adding artificial viscosity terms in the equations, following Wilson's approach. Evans [57] was able to show that Newtonian gravity and the quadrupole formula for gravitational radiation were inadequate to study the problem.

Most of the aforementioned axisymmetric codes adopted spherical polar coordinates. Numerical instabilities are encountered at the origin ($r = 0$) and, mainly, at the polar axis ($\theta = 0, \pi$) where some fields diverge due to the coordinate singularities. Evans did important contributions towards regularizing the gravitational field equations in such situations [57]. These coordinate problems have refrained researchers from building three-dimensional codes in spherical coordinates. In this case Cartesian coordinates are adopted which, despite the desired property of being everywhere regular, present the important drawback of not being adapted to the topology of astrophysical systems. As a result this has important consequences on the grid resolution requirements. The only extension of an axisymmetric 3+1 code using spherical coordinates to three dimensions has been accomplished by Stark [187] although no applications in relativistic astrophysics have yet been presented.

Alternatively, existing axisymmetric codes employing the characteristic formulation of the Einstein equations [209], as the (vacuum) one presented in [75], do not share the axis instability problems of spacelike codes. Hence, axisym-

[2]Müller [131] obtained the first numerical evidence of the low gravitational efficiency of the core-collapse scenario. By means of axisymmetric Newtonian simulations he found that $E < 10^{-6} Mc^2$ was radiated as gravitational waves.

metric characteristic codes, once conveniently coupled to matter fields, could be a promising way of studying the axisymmetric collapse problem.

In a much simpler approach some investigations have considered dynamical evolutions of a collisionless gas of particles in full general relativity [176, 177, 178, 179, 1]. Such pressureless particles move along geodesics of the spacetime. The geodesic equations are, in comparison to the hydrodynamic equations, trivial to integrate. All efforts can focus, then, on solving the gravitational field equations. Shapiro and Teukolsky [176, 177] built a code to solve the Vlasov equation in general relativity by N-body particle simulation, computing the gravitational field using the ADM formalism. They studied the origin of quasars and active galactic nuclei via the collapse of relativistic star clusters to supermassive black holes. They also considered the collapse of prolate spheroids finding that if those are sufficiently compact, the final singularities are hidden inside black holes. On the controversial side, however, they found that when the spheroids are large enough there are no apparent horizons, in disagreement with the cosmic censorship hypothesis [155] because a naked singularity may form in non-spherical relativistic collapse. Collapses with small enough angular momentum also showed the same behavior. Such computations have not yet been attempted using a fully hydrodynamical code.

Semi-analytical studies of finite-sized collections of dust, shaped in the form of stars or shells, falling isotropically onto a black hole are available in the literature [137, 81, 180, 145, 157]. These investigations approximate gravitational collapse by a dust shell of mass m falling into a Schwarzschild black hole of mass $M \gg m$. These studies have shown that for a fixed amount of infalling mass the gravitational radiation efficiency is reduced compared to the point particle limit, never exceeding that of a particle with the same mass, the reason being cancellations of the emission from distinct parts of the extended object.

In [151] such conclusions were corroborated with a numerical simulation of the gravitational radiation emitted during the accretion process of an extended object on to a black hole. The first order deviations from the exact black hole geometry were approximated using curvature perturbations induced by matter sources whose non-linear evolution was integrated using a (non-linear) hydrodynamical code (adopting Valencia's conservative formulation and HRSC schemes). All possible types of curvature perturbations are captured in the real and imaginary parts of the Weyl tensor scalar (see, e.g., [41]). In the framework of the Newman-Penrose formalism the equations for the perturbed Weyl tensor components decouple, and when written in the frequency domain even separate [193]. Papadopoulos and Font [151] used the limiting case for Schwarzschild black holes, i.e., the inhomogeneous Bardeen-Press equation [14]. The simulations showed the gradual excitation of the black hole quasi-normal mode frequency by sufficiently compact shells.

An example of these simulations appears in MPEG movie 2 of Fig. 6 (only an intermediate snapshot of the evolution is depicted in the figure). This movie shows the time evolution of the shell density (left panel) and the asso-

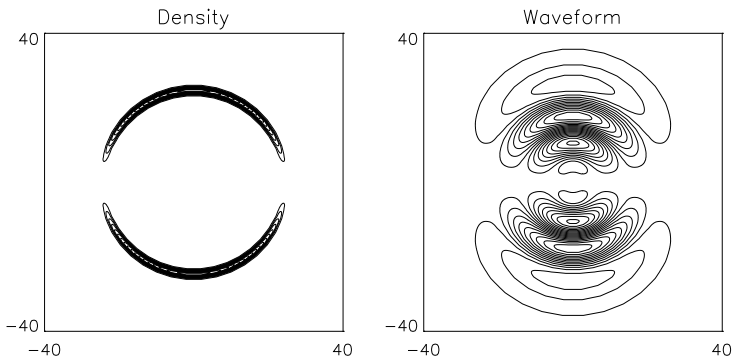

Figure 6: MPEG 2. Time evolution of the accretion/collapse of a quadrupolar shell on to a Schwarzshild black hole (*the figure only shows an arbitrary snapshot*). The left panel shows isodensity contours and the right panel the associated gravitational waveform. The shell, initially centered at $r_* = 35M$, is gradually accreted by the black hole, a process which perturbs the black hole and triggers the emission of gravitational radiation. After the burst, the remaining evolution shows the decay of the black hole quasi-normal mode ringing. By the end of the simulation a spherical accretion solution is reached. Further details are given in [151].

ciated gravitational waveform during a complete accretion/collapse event. The (quadrupolar) shell is parametrized according to $\rho = \rho_0 + e^{-k(r_*-r_0)^2}\sin^2\theta$ with $k = 2, \rho_0 = 10^{-2}$ and $r_0 = 35M$. Additionally r_* denotes a logarithm radial (Schwarzschild) coordinate. The animation shows the gradual collapse of the shell on to the black hole. This process triggers the emission of gravitational radiation. In the movie it can be clearly seen how the burst of the emission coincides with the more dynamical accretion phase, when the shell crosses the peak of the potential and is subsequently captured by the hole. The gravitational wave signal coincides with the quasinormal ringing frequency of the black hole, $17M$. The existence of an initial burst, causally separated from the *physical* burst, is also noticeable in the movie. It just reflects the gravitational radiation content of the initial data (see [151] for a detailed explanation).

We end this section pointing out that, to date, there are no three-dimensional relativistic simulations of gravitational collapse yet available. All the existing computations have been done using Newtonian physics. Bonazzola and Marck [29] performed the first three-dimensional simulations, using pseudo-spectral methods, very accurate and free of numerical or intrinsic viscosity.

They confirmed the low amount of energy radiated in gravitational waves regardless of the initial conditions of the collapse: axisymmetric, rotating or tidally deformed. Their results are only applicable to the pre-bounce phase of the supernova collapse as the simulations do not consider shock propagation after bounce.

The more detailed multi-dimensional non-relativistic simulations are those performed by the MPA/Garching group (an on-line sample can be found at the URL address `http://www.mpa-garching.mpg.de/Hydro/hydro.html`). As mentioned before these include sophisticated microphysics and employ accurate HRSC integration schemes. To illustrate the degree of sophistication achieved in Newtonian simulations we present in MPEG movie 3 an animation of the early evolution of a core collapse supernova explosion up to 220 ms after core bounce and shock formation (only an intermediate snapshot at 130 ms is depicted in Fig. 7). The movie shows the evolution of the entropy within the innermost 3000 km of the star.

The initial data used in these calculations is taken from the $15\,M_\odot$ pre-collapse model of a blue supergiant star of [212]. The computations start 20 ms after core bounce, from a one-dimensional model of [37]. This model is obtained with the one-dimensional general relativistic code mentioned previously [35] which includes a detailed treatment of the neutrino physics and a realistic EOS, and which is able to follow core collapse, bounce and the associated formation of the supernova shock. Because of neutrino cooling and energy losses due to the dissociation of iron nuclei the shock initially stalls inside the iron core.

The movie shows how the stalling shock is "revived" by neutrinos streaming from the outer layers of the hot, nascent neutron star in the center. This leads to a net heating and a negative entropy gradient in the region between the so called "gain-radius" at about 100 km and the shock farther outwards where convective instabilities set in. They are characterized by large rising blobs of neutrino heated matter and cool, narrow downflows. The convective energy transport increases the efficiency of energy deposition in the post-shock region by transporting heated material near the shock and cooler matter near the gain radius where the heating is strongest. The freshly heated matter then rises again while the shock is distorted by the upward streaming bubbles. The reader is addressed to [97] for a more detailed description of a more energetic initial model.

4.2 Accretion on to black holes

The study of relativistic accretion and black hole astrophysics is currently a very active field of research, both theoretically and observationally (see, e.g., [23] and references there in). Advances in satellite instrumentation, e.g., the Rossi X-Ray Timing Explorer (RXTE), and the Advanced Satellite for Cosmology and Astrophysics (ASCA), are greatly stimulating and guiding theoretical research on accretion physics. The recent discovery of kHz quasi-periodic oscillations in

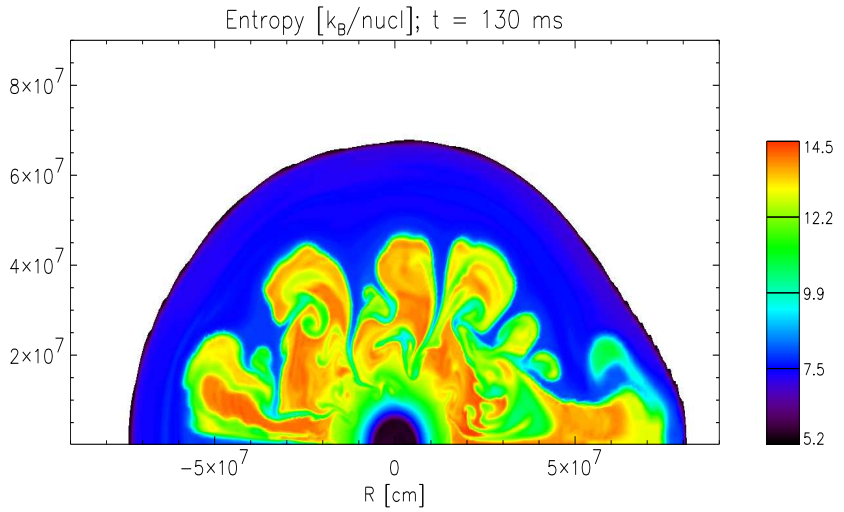

Figure 7: MPEG 3. Animation of the time evolution of the entropy in a core collapse supernova explosion [97] (*in the figure only an snapshot of the evolution is depicted, at* $t = 130ms$). The movie shows the evolution within the innermost 3000 km of the star and up to 220 ms after core bounce. See text for explanation.

low-mass X-ray binaries, extends the frequency range over which these oscillations occur into timescales associated with the innermost regions of the accretion process (for a review see [195]). Moreover, in extragalactic sources, spectroscopic evidence (broad iron emission lines) increasingly points to (rotating) black holes being the accreting central objects [192, 100, 34].

Additionally, most of the proposed theoretical models to explain γ-ray bursts involve a, possibly hyper-accreting, black hole at some point of the evolutionary paths [160]: neutron star-neutron star and black hole-neutron star binaries, collapsars, black hole-white dwarf binaries or common envelope evolution of compact binary systems. Developing the capability of performing accurate numerical simulations of time-dependent accretion flows in regions of strong gravitational fields, possibly dynamic during the hyper-accreting phase, is indeed enormously motivated.

Accretion theory is primarily based on the study of (viscous) stationary flows and their stability properties through linearized perturbations thereof. A well-known example are the unstable, to a variety of non-axisymmetric global modes, isentropic constant angular momentum tori as discovered by Papaloizou and Pringle [153] (see [10] for a review of instabilities in astrophysical accretion disks). Establishing the nature of flow instabilities requires highly resolved and accurate, time-dependent, non-linear numerical investigations in strong black

hole gravitational fields. Such simulations have only been attempted, in general relativity, in a few cases and only for inviscid flows.

For a wide range of accretion problems, a Newtonian theory of gravity is adequate for the description of the background gravitational forces (see, e.g., [68]). The extensive experience with Newtonian astrophysics suggests that the first explorations of the relativistic regime could benefit from the use of model potentials [149]. For comprehensive numerical work, a full (i.e., three-dimensional) formalism is required, able to cover also the maximally rotating hole. In rotating spacetimes the gravitational forces cannot be captured fully with scalar potential formalisms. Additionally, geometric regions such as the ergo-sphere would be very hard to model without a metric description. Whereas the bulk of emission occurs in regions with almost Newtonian fields, only the observable features attributed to the inner region may crucially depend on the nature of the spacetime.

In the following we present a summary of illustrative time-dependent accretion simulations in relativistic hydrodynamics. We concentrate on multi-dimensional simulations. In the limit of spherical accretion exact stationary solutions exist for both, Newtonian gravity [30] and relativistic gravity [123]. Such solutions are commonly used as test-beds of time-dependent hydrodynamical codes, by analizing whether stationarity is maintained during a numerical evolution [85, 112, 56, 165, 12].

4.2.1 Time-dependent disk accretion simulations

Pioneering numerical efforts in the study of black hole accretion [203, 85, 82, 83] made use of the the so-called *frozen star* paradigm of a black hole. In this framework, the time "slicing" of the spacetime is synchronized with that of asymptotic observers far from the hole. Within this approach Wilson [203] first investigated numerically the time-dependent accretion of inviscid matter onto a rotating (Kerr) black hole. This was the first problem to which his formulation of the hydrodynamic equations, as presented in Section 2.1.2, was applied. Wilson used an axisymmetric hydrodynamical code in cylindrical coordinates studying the formation of shock waves and the X-ray emission in the strong-field regions close to the black hole horizon, being able to follow the formation of thick accretion disks during the simulations.

Wilson's formulation has been extensively used in time-dependent numerical simulations of disk accretion. In [85] (see also [82]) Hawley and collaborators studied, in the test-fluid approximation and axisymmetry, the evolution and development of non-linear instabilities in pressure-supported accretion disks formed as a consequence of the spiraling infall of fluid with some amount of angular momentum. Their initial models were computed following the analytic theory of relativistic disks presented by [2]. The code used explicit second-order finite difference schemes with a variety of choices to integrate the transport terms of the equations (i.e., those involving changes in the state of the fluid at

a specific volume in space). The code also used a staggered grid (with scalars located at the cell centers and vectors at the cell boundaries) for its suitability to difference the transport equations. Discontinuous solutions were stabilized with artificial viscosity terms.

With a three-dimensional extension of the axisymmetric code of [84, 85] Hawley [83] studied the global hydrodynamic non-axisymmetric instabilities in thick, constant angular momentum accretion gas tori orbiting around a Schwarzschild black hole. Such simulations showed that in radially wide, nearly constant angular momentum tori, the Papaloizu-Pringle instability saturates in a strong spiral pressure wave, not in turbulence. In addition, the simulations confirmed that accretion flows through the torus could reduce and even halt the growth of the global instability.

Igumenshchev and Beloborodov [92] have performed two-dimensional relativistic hydrodynamical simulations of inviscid transonic disk accretion on to a rotating (Kerr) black hole. The hydrodynamical equations follow Wilson's formulation but the code avoids the use of artificial viscosity. The advection terms are evaluated with an upwind algorithm which incorporates the PPM scheme [44] to compute the fluxes. Their numerical work confirms analytical expectations: (i) the structure of the innermost disc region strongly depends on the black hole spin and (ii) the mass accretion rate goes as $\dot{M} \propto (\Delta W)^{\Gamma/(\Gamma-1)}$, ΔW being the energy gap at the cusp of the torus (i.e. $\Delta W = W_0 - W_{\rm cusp}$, W_0 being the potential at the boundary of the torus) and Γ the adiabatic index.

Yokosawa [214, 215], also using Wilson's formulation, studied the structure and dynamics of relativistic accretion disks and the transport of energy and angular momentum in magnetohydrodynamical accretion on to a rotating black hole. In his code the hydrodynamic equations are solved using the Flux-Corrected-Transport (FCT) scheme [33] (a second-order flux-limiter method in smooth regions which avoids oscillations near discontinuities by reducing the magnitude of the numerical flux) and the magnetic induction equation is solved using the constrained transport method [58]. The code contains a parametrized viscosity based on the α-model. The simulations revealed different flow patterns, inside the marginally stable orbit, depending on the thickness, h, of the accretion disk. For thick disks with $h \geq 4r_h$, r_h being the radius of the event horizon, the flow pattern becomes turbulent.

4.2.2 Wind accretion simulations

The term "wind" or hydrodynamic accretion refers to the capture of matter by a moving object under the effect of the underlying gravitational field. The canonical astrophysical scenario in which matter is accreted in such a non-spherical way was suggested originally by Bondi, Hoyle and Lyttleton [87, 31], who studied, using Newtonian gravity, the accretion on to a gravitating point mass moving with constant velocity through a non-relativistic gas of uniform density. The matter flow inside the accretion radius, after being decelerated

by a conical shock is ultimately captured by the central object. Such process applies to describe mass transfer and accretion in compact X-ray binaries, in particular in the case in which the donor (giant) star lies inside its Roche lobe and loses mass via a stellar wind. This wind impacts on the orbiting compact star forming a bow-shaped shock front around it. Such an accretion process is also thought to take place during common envelope evolution of a binary system.

Since those analytic studies numerical simulations by an increasing number of authors (see, e.g., [166, 19] and references therein) extended the simplified analytic models and helped develop a thorough understanding of the hydrodynamic accretion scenario, in its fully three-dimensional character. These investigations revealed the formation of accretion disks and the appearance of non-trivial phenomena such as shock waves or *flip-flop* (tangential) instabilities.

Most of the existing numerical work has used Newtonian hydrodynamics, to study the accretion on to non-relativistic stars. For compact accretors such as neutron stars or black holes the correct numerical modeling requires a general relativistic hydrodynamical description. Within the relativistic, frozen star, framework wind accretion on to "moving" black holes was first studied in axisymmetry by [156]. In this work Wilson's formulation of the hydrodynamic equations was adopted. The integration algorithm was taken from [189] with the transport terms finite-differenced following the prescription given in [85]. An artificial viscosity term of the form $Q = a\rho(\Delta v)^2$, with a a constant, was added to the pressure terms of the equations.

More recently, an extensive survey of the morphology and dynamics of relativistic wind accretion past a Schwarzschild black hole was performed in [63, 62]. This investigation differs from [156] in both, the use of a conservative formulation for the hydrodynamic equations (Valencia's formulation; see Section 2.1.3) and the use of advanced HRSC schemes. Axisymmetric computations were compared to [156] finding major differences in the shock location, opening angle and accretion rates of mass and momentum. The reasons for the discrepancies may be diverse and related to the use of different formulations, numerical schemes and, possibly, to the grid resolution. In [156] canonical grid sizes were extremely coarse, of 40×20 zones in r and $\cos\theta$ respectively. The simulations presented in [63, 62] used much finer grids in every direction.

Non-axisymmetric two-dimensional studies, restricted to the equatorial plane of the black hole, were first performed in [62], motivated by the non-stationary patterns found in Newtonian simulations (see, e.g., [19]). The relativistic computations revealed that initially asymptotic uniform flows always accrete on to the hole in a stationary way which closely resembles the previous axisymmetric patterns.

Papadopoulos and Font [150] have recently presented a procedure which considerably simplifies the integration of the general relativistic hydrodynamic equations near black holes. Their procedure is based on identifying classes of coordinates in which the black hole metric is free of coordinate singularities at

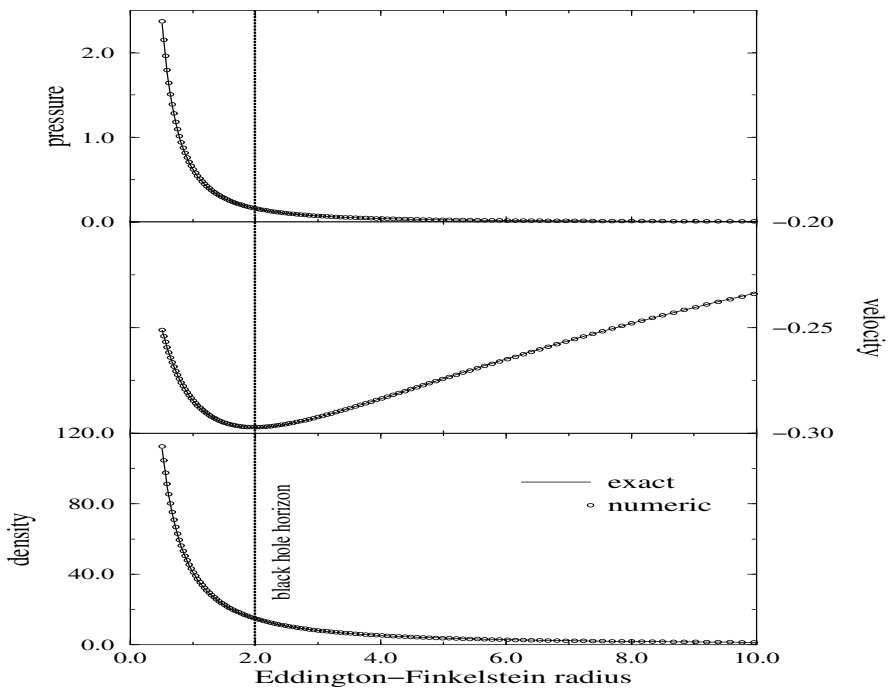

Figure 8: Exact (solid line) versus numerical (circles) solution for spherical accretion of a perfect fluid in Eddington-Finkelstein coordinates [150]. The solution extends inside the event horizon of the black hole, at $r = 2M$, where all fields are smooth, only blowing up at the central singularity, at $r = 0$.

the horizon (unlike the commonly adopted Boyer-Lindquist coordinates), independent of time, and admits a spacelike decomposition. With those coordinates the innermost radial boundary can be placed *inside* the horizon, allowing for a clean treatment of the entire (exterior) physical domain. In [150] Michel (spherical) solution was re-derived using a particular coordinate system adapted to the black hole horizon, the Eddington-Finkelstein system. In Fig. 8 a representative sample of hydrodynamical quantities are plotted for this stationary solution. The solid lines correspond to the exact solution and the symbols correspond to the numerical solution. The solution is regular well inside the horizon at $r = 2M$. The steepness of the hydrodynamic quantities dominates the solution only near the real singularity.

In [65, 66] this approach was applied to the study of relativistic wind accretion on to rapidly rotating (Kerr) black holes. The effects of the black hole

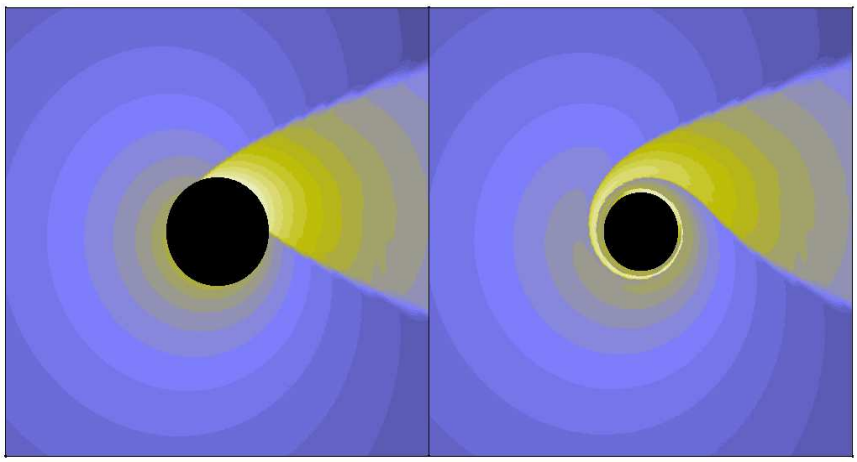

Figure 9: Relativistic wind accretion onto a rapidly rotating Kerr black hole ($a = 0.999M$, the hole spin is counter-clock wise) in Kerr-Schild coordinates (left panel). Isocontours of the logarithm of the density are plotted at the final stationary time $t = 500M$. Brighter colors (yellow-white) indicate high density regions while darker colors (blue) correspond to low density zones. The right panel shows how the flow solution looks like when transformed to Boyer-Lindquist coordinates. The shock appears here totally wrapped around the horizon of the black hole. The box is $12M$ units long. The simulation employed a (r, ϕ)-grid of 200×160 zones. Further details are given in [65].

spin on the flow morphology were found to be confined to the inner regions of the black hole potential well. Within this region, the black hole angular momentum drags the flow, wrapping the shock structure around. An illustrative example appears depicted in Fig. 9. The left panel of this figure corresponds to a simulation employing the Kerr-Schild form of the Kerr metric, regular at the horizon. The right panel shows how the accretion pattern would look like were the computation performed using the more common Boyer-Lindquist coordinates. The transformation induces a noticeable wrapping of the shock around the central hole. The shock would wrap infinitely many times before reaching the horizon. As a result, the computation in these coordinates would be much more challenging than in Kerr-Schild coordinates.

4.3 Hydrodynamical evolution of neutron stars

The numerical evolution of neutron stars in general relativity is nowadays a very active field of research [183, 117, 67, 126, 181, 61]. The numerical investigation of many interesting astrophysical processes involving neutron stars, such as the rotational evolution of proto-neutron stars or the gravitational radiation from unstable pulsation modes or, more importantly, from the catastrophic coalescence and merge of neutron star-neutron star or black hole-neutron star binaries, requires the ability of accurate, long-term hydrodynamical evolutions employing relativistic gravity.

Evolutions of polytropic models of spherical neutron stars (i.e., with EOS $p = K\rho^{\Gamma}$, K being the polytropic constant) using relativistic hydrodynamics can be used as test-bed computations for multidimensional codes. One-dimensional hydrodynamical studies of relativistic stars have been preformed by [77], employing pseudo-spectral methods, and by [165] with HRSC schemes. These investigations adopted radial gauge polar slicing coordinates in which the general relativistic equations are expressed in a simple way which resembles Newtonian hydrodynamics. Gourgoulhon [77] used a numerical code to detect, dynamically, the zero value of the fundamental mode of a neutron star against radial oscillations. Romero et al [165] highlighted the accuracy of HRSC schemes by finding, numerically, a change in the stability behavior of two slightly different initial neutron star models: a model with mass $1.94532 M_{\odot}$ is stable and a model of $1.94518 M_{\odot}$ is unstable.

Three-dimensional hydrodynamical evolutions of relativistic, self-gravitating neutron stars have been considered in [67, 181, 3, 61]. In [67] a new efficient, parallel, general relativistic hydrodynamical code was presented and thoroughly tested. In this code, Valencia's hydrodynamical (conservative) formulation was adopted and a variety of state-of-the-art Riemann solvers were implemented, including Roe's solver [164] and Marquina's flux formula [49]. The Einstein equations were formulated using two different approaches: (i) the standard ADM formalism and (ii) a hyperbolic formulation developed in [27]. The code was subjected to a series of convergence tests, with (twelve) different combinations of the spacetime and hydrodynamics finite differencing schemes, demonstrating the consistency of the discrete equations with the differential equations. The simulations performed in [67] include, among others, the evolution of equilibrium configurations of compact stars (solutions to the TOV equations), and the evolution of relativistically boosted TOV stars ($v = 0.3c$) transversing diagonally across the computational domain. In the long term plan this code is designed to simulate the inspiral coalescence of two neutron stars in general relativity. The more "academic" scenario of a head-on collision has been already analyzed in [126] and is briefly described below.

The simulations presented in [181, 3, 61] are performed using a recent reformulation of the ADM equations proposed by [17] based upon a conformal decomposition of the three metric and extrinsic curvature. This formulation has

proved to be much more long-term stable (though somehow less accurate, see [3]) than standard ADM. The tests analyzed include evolutions of weak gravitational waves [17], self-gravitating matter configurations with prescribed (analytic) time evolution [16], spherical dust collapse [181], strong gravitational waves (which even collapse to black holes) [3], black holes [3] and boson stars [3]. Hydrodynamical evolutions of neutron stars are extensively considered in [181, 61].

Nowadays, most of the current efforts in developing codes in relativistic astrophysics are strongly motivated by the simulation of the coalescence of compact binaries. These scenarios are considerered the most promising sources of gravitational radiation to be detected by the planned laser interferometers going online worldwide in the next few years. The computation of the gravitational wave during the most dynamical phase of the coalescence stage depends crucially on hydrodynamical, finite-size, effects. This phase begins once the stars, initially in quasi-equilibrium orbits of gradually smaller orbital radius, due to the emission of gravitational waves, reach the innermost stable circular orbit (see the schematic plot in Fig. 10). From here on, the final merge of the two objects takes place in a dynamical timescale and lasts for a few milliseconds. A Newtonian treatment of this stage would be valid as long as $M/R \ll 1$ and $M/r \ll 1$ simultaneously, M being the mass of the binary, R the neutron star radius and r the separation of the two stars. As the stars gradually approach each other and merge both inequalities are less valid and relativistic calculations become necessary.

The accurate simulation of a binary neutron star coalescence is however one of the most challenging tasks in numerical relativity. These scenarios involve strong gravitational fields, matter motion with (ultra) relativistic speeds and/or strong shock waves. The difficulties for a succesful numerical integration are exacerbated by the intrinsic multidimensional character of the problem and by the inherent complexities in Einstein theory of gravity, e.g., coordinate degrees of freedom and the possible formation of curvature singularities (e.g., collapse of matter configurations to black holes).

For these reasons it is not surprising that most of the available simulations have been attempted in the Newtonian (and post-Newtonian) framework. Most of these studies employ Lagrangian particle methods such as SPH and only a few have considered (less viscous) high-order finite difference methods such as PPM [167]. The interested reader is referred to the recent reviews by Swesty [190] and Rasio and Shapiro [161] for detailed descriptions of the current status of Newtonian simulations.

Concerning relativistic simulations Wilson's hydrodynamical formulation has been applied to the study of neutron star binary coalescence in [207, 208] under the assumption of a conformally flat spacetime, which leads to a considerable simplification of the gravitational field equations. In this case they reduce to a coupled set of elliptic (Poison-like) equations for the lapse function, shift vector and conformal factor. Their simulations revealed, unexpectedly, the appearance of a "binary-induced collapse instability" of the neutron stars, prior to the

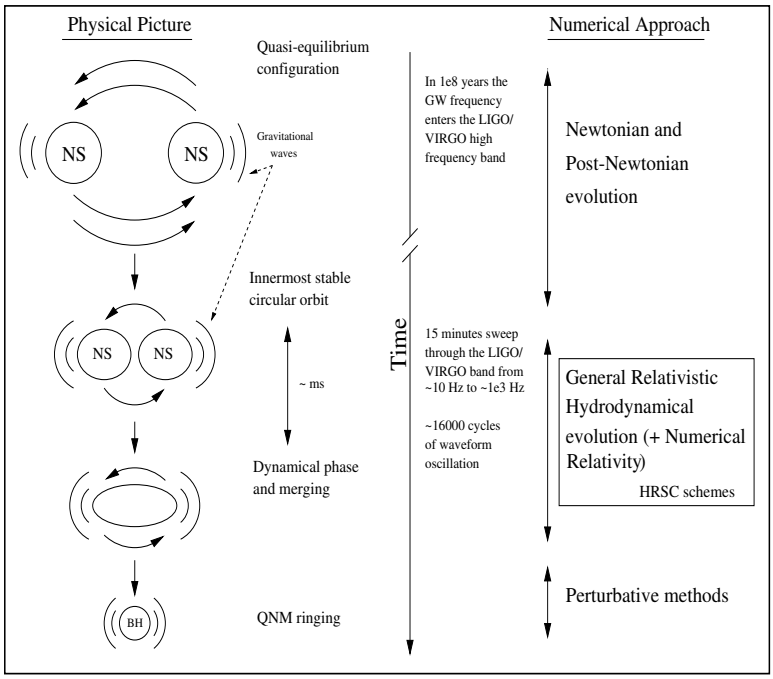

Figure 10: Schematic graph showing the evolution of a neutron star binary (left side) together with the numerical approach (right side) best suited for an accurate description of each portion of the evolution. General relativistic hydrodynamic simulations are unavoidable during the most dynamical phase from the innermost stable circular orbit to the final merge.

eventual collapse of the final merged object, with the central density of each star increasing by an amount proportional to $1/r$. The numerical results of Wilson and collaborators have been criticized by many authors on theoretical grounds (see references in [161] for un updated discussion). Reliable numerical simulations with the full set of Einstein equations will ultimately clarify these results.

Nakamura and co-workers are embarked in a programme to simulate neutron star binary coalescence in general relativity since the late 80's (see, e.g., [136]). A three-dimensional code employing the full set of Einstein equations and self-gravitating matter fields has been developed [146]. In this code the complete set of the equations, spacetime and hydrodynamics, are finite-differenced in a uniform Cartesian grid using van Leer's scheme [196] with TVD flux limiters. Shock waves are spread out using a tensor artificial viscosity algorithm. The hydrodynamic equations follow Wilson's formulation and the ADM formalism is adopted for the Einstein equations. This code has been tested in the study

of the gravitational collapse of a rotating polytrope to a black hole (comparing to the axisymmetric computation of [188]) and applied to the coalescence of a binary neutron star system. Further work to achieve long term stability is currently under way [146].

The most advanced simulations of neutron star coalescence in full general relativity are those reported recently by Shibata [181]. His code is able to simulate a coalescence event for a long time from the innermost circular orbit up to the formation of a final merged object (either a black hole or a neutron star). The code shares many features with that of [146]: the hydrodynamic equations are formulated following Wilson's approach and they are solved using van Leer's [196] second order finite difference scheme with artificial viscosity. The most important difference concerns the reformulation of the ADM Einstein equations into a conformal traceless system [3]. Shibata computed the merger of two models of corotating binary neutron stars of $\Gamma = 5/3$ in contact and in approximate quasi-equilibrium orbits. The central density of each star in the two models was 6×10^{-4} (mildly relativistic) and 10^{-3}, in natural units. The quasi-equilibrium models are constructed assuming a polytropic EOS with $K = 10$. For both initial models, at half the orbital period P of the quasi-equilibrium states the neutron stars begin to merge forming spiral arms, and by $t \approx 1.5P$ the final object is a rapidly and differentially rotating, highly flattened neutron star. For the more relativistic model the central density of the merged object is $\approx 1.4 \times 10^{-3}$, which is nearly the maximum allowed density along the sequence of stable neutron stars of $K = 10$ and $\Gamma = 5/3$. Hence, a black hole could be formed directly in the merger of initially more massive neutron stars. For the cases considered by Shibata, the new star is strongly supported by rapid rotation ($J/M_g^2 \approx 1$, J being the angular momentum and M_g the gravitational mass) and could eventually collapse to a black hole once sufficient angular momentum has dissipated through, e.g., neutrino emission or gravitational radiation.

Recently [126] have studied the head-on collision of two neutron stars by means of time-dependent relativistic simulations using the code of [67]. These simulations are aimed to investigate whether the collapse of the final object occurs in prompt or delayed (after neutrino cooling) timescales. Prompt collapse to a black hole was found in the head-on collision of two $1.4M_\odot$ neutron stars modeled by a polytropic EOS with $\Gamma = 2$ and $K = 1.16 \times 10^5 cm^5/g\,s^2$. The stars are initially separated by a proper distance of $d = 44$km and are boosted towards one another at a speed of $\sqrt{GM/d}$ (the Newtonian infall velocity). The simulation employed a Cartesian grid of 192^3 points. The time evolution of this simulation can be followed in Quicktime movie 4 (the first snapshot of this movie is depicted in Fig. 11). This animation shows, simultaneously, the rest-mass density and the internal energy evolution during the on-axis collision. The formation of the black hole in prompt timescales is demonstrated by the

[3] This formulation was originally introduced by Shibata and Nakamura [182] and recently slightly modified by [17].

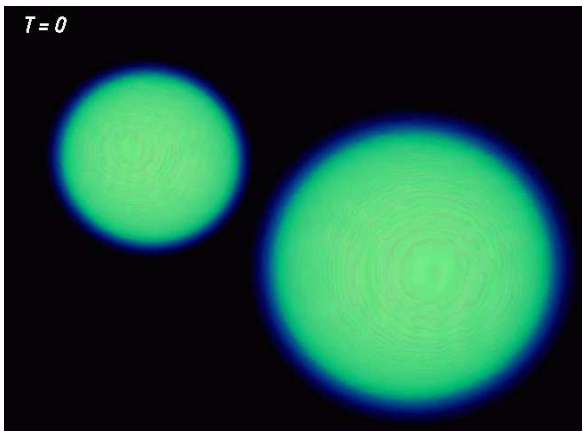

Figure 11: Animation of a head-on collision simulation of two $1.4M_\odot$ neutron stars obtained with a relativistic code [67, 126] (*the figure only shows the intial configuration*). The movie shows the evolution of the density and internal energy. The formation of the black hole in prompt timescales is demonstrated by the sudden appearance of the apparent horizon at $t = 0.16ms$ ($t = 63.194$ in code units), which is indicated by violet dotted circles representing the trapped photons.

sudden appearance of the apparent horizon at $t = 0.16ms$ ($t = 63.194$ in code units). The violet dotted circles indicate the trapped photons. The animation also shows a moderately relativistic shock wave (Lorentz factor of about 1.2) appearing at $t \approx 36$ (code units; yellow-white colors) which eventually is followed by two opposite moving shocks (along the infalling z direction) which propagate along the black hole surrounding atmosphere.

5 Additional information

This last section of the review contains technical information concerning recent developments for the implementation of Riemann solver based numerical schemes in general relativistic hydrodynamics.

5.1 Riemann problems in locally Minkowskian coordinates

In [159] a procedure to integrate the general relativistic hydrodynamic equations (as formulated in Section 2.1.3), taking advantage of the multitude of Riemann solvers developed in Special Relativity, was presented. The approach relies on a local change of coordinates in terms of which the spacetime metric is locally Minkowskian. This procedure allows, for 1D problems, to use the exact solution

of the special relativistic Riemann problem [114].

Such a coordinate transformation to locally Minkowskian coordinates at each numerical interface, assumes that the solution of the Riemann problem is the one in special relativity and planar symmetry. This last assumption is equivalent to the approach followed in classical fluid dynamics, when using the solution of Riemann problems in slab symmetry for problems in cylindrical or spherical coordinates, which breaks down near the singular points (e.g., the polar axis in cylindrical coordinates). In analogy to classical fluid dynamics, the numerical error depends on the magnitude of the Christoffel symbols, which might be large whenever huge gradients or large temporal variations of the gravitational field are present. Finer grids and improved time advancing methods will be required in those circumstances.

Following [159] we illustrate the procedure computing the second flux integral in Eq. (46), which we call $\mathcal{I}$. We begin by expressing the integral on a basis $\mathbf{e}_{\hat{\alpha}}$ with $\mathbf{e}_{\hat{0}} \equiv n^{\mu}$ and $\mathbf{e}_{\hat{i}}$ forming an orthonormal basis in the plane orthogonal to n^{μ} with $\mathbf{e}_{\hat{1}}$ normal to the surface Σ_{x^1} and $\mathbf{e}_{\hat{2}}$ and $\mathbf{e}_{\hat{3}}$ tangent to that surface. The vectors of this basis verify $\mathbf{e}_{\hat{\alpha}} \cdot \mathbf{e}_{\hat{\beta}} = \eta_{\hat{\alpha}\hat{\beta}}$ with $\eta_{\hat{\alpha}\hat{\beta}}$ the Minkowski metric (in the following, caret subscripts will refer to vector components in this basis).

Denoting by x_0^{α} the coordinates at the center of the interface at time t, we introduce the following locally Minkowskian coordinate system $x^{\hat{\alpha}} = M^{\hat{\alpha}}_{\alpha}(x^{\alpha} - x_0^{\alpha})$, where the matrix $M^{\hat{\alpha}}_{\alpha}$ is given by $\partial_{\alpha} = M^{\hat{\alpha}}_{\alpha}\mathbf{e}_{\hat{\alpha}}$, calculated at x_0^{α}. In this system of coordinates the equations of general relativistic hydrodynamics transform into the equations of special relativistic hydrodynamics, in Cartesian coordinates, but with non-zero sources, and the flux integral reads

$$\mathcal{I} \equiv \int_{\Sigma_{x^1}} \sqrt{-g} F^1 dx^0 dx^2 dx^3 = \int_{\Sigma_{x^1}} \left(F^{\hat{1}} - \frac{\beta^{\hat{1}}}{\alpha} F^{\hat{0}} \right) \sqrt{-\hat{g}}\, dx^{\hat{0}} dx^{\hat{2}} dx^{\hat{3}} \qquad (61)$$

(the caret symbol representing the numerical flux in Eq. (46) is now removed to avoid confusion) with $\sqrt{-\hat{g}} = 1 + \mathcal{O}(x^{\hat{\alpha}})$, where we have taken into account that, in the coordinates $x^{\hat{\alpha}}$, Σ_{x^1} is described by the equation $x^{\hat{1}} - \frac{\beta^{\hat{1}}}{\alpha} x^{\hat{0}} = 0$ (with $\beta^{\hat{i}} = M^{\hat{i}}_i \beta^i$), where the metric elements β^1 and α are calculated at x_0^{α}. Therefore, this surface is not at rest but moves with *speed* $\beta^{\hat{1}}/\alpha$.

At this point all the theoretical work on special relativistic Riemann solvers developed in recent years, can be exploited. The quantity in parenthesis in Eq. (61) represents the numerical flux across Σ_{x^1}, which can, now, be calculated by solving the special relativistic Riemann problem defined with the values at the two sides of Σ_{x^1} of two independent thermodynamical variables (namely, the rest mass density ρ and the specific internal energy ε) and the components of the velocity in the orthonormal spatial basis $v^{\hat{i}}$ ($v^{\hat{i}} = M^{\hat{i}}_i v^i$).

Once the Riemann problem has been solved, we can take advantage of the self-similar character of the solution of the Riemann problem, which makes it constant on the surface Σ_{x^1} simplifying the calculation of the above integral

enormously:

$$\mathcal{I} = \left(F^{\hat{1}} - \frac{\beta^{\hat{1}}}{\alpha} F^{\hat{0}} \right)^{*} \int_{\Sigma_{x^1}} \sqrt{-\hat{g}}\, dx^{\hat{0}} dx^{\hat{2}} dx^{\hat{3}} \tag{62}$$

where the superscript (*) stands for the value on Σ_{x^1} obtained from the solution of the Riemann problem. Notice that the numerical fluxes correspond to the vector fields $F^1 = \{\mathbf{J},\, \mathbf{T}\cdot\mathbf{n},\, \mathbf{T}\cdot e_{\hat{1}},\, \mathbf{T}\cdot e_{\hat{2}},\, \mathbf{T}\cdot e_{\hat{3}}\}$ and linearized Riemann solvers provide the numerical fluxes as defined in Eq. (61). Thus the additional relation $\mathbf{T}\cdot\partial_i = M_i^{\hat{j}}(\mathbf{T}\cdot\mathbf{e}_{\hat{j}})$ has to be used for the momentum equations. The integral in the right hand side of Eq. (62) is the area of the surface Σ_{x^1} and can be expressed in terms of the original coordinates as

$$\int_{\Sigma_{x^1}} \sqrt{-\hat{g}}\, dx^{\hat{0}} dx^{\hat{2}} dx^{\hat{3}} = \int_{\Sigma_{x^1}} \sqrt{\gamma^{11}}\sqrt{-g}\, dx^0 dx^2 dx^3 \tag{63}$$

which can be evaluated for a given metric. The interested reader is addressed to [159] for details on the testing and calibration of this procedure.

5.2 Characteristic fields in Valencia's general relativistic hydrodynamics formulation

This section collects all information concerning the characteristic structure of the general relativistic hydrodynamic equations in Valencia's formulation (Section 2.1.3). As explained in Section 3.1.2 this information is necessary in order to implement approximate Riemann solvers in HRSC finite difference schemes.

We only present the characteristic speeds and fields corresponding to the x-direction. Equivalent expressions for the two other directions can be easily obtained by symmetry considerations. The characteristic speeds (eigenvalues) of the system are given by:

$$\lambda_0 = \alpha v^x - \beta^x \qquad \text{(triple)}, \tag{64}$$

$$\lambda_\pm = \frac{\alpha}{1-v^2c_s^2}\left\{ v^x(1-c_s^2) \pm c_s\sqrt{(1-v^2)[\gamma^{xx}(1-v^2c_s^2) - v^x v^x(1-c_s^2)]}\right\} - \beta^x, \tag{65}$$

where c_s denotes the local sound speed, which can be obtained from $hc_s^2 = \chi + \frac{p}{\rho^2}\kappa$, with $\chi \equiv \frac{\partial p}{\partial \rho}$ and $\kappa \equiv \frac{\partial p}{\partial \varepsilon}$. We note that the Minkowskian limit of these expressions is properly recovered (see [48]) as well as the Newtonian one ($\lambda_0 = v^x$, $\lambda_\pm = v^x \pm c_s$).

A complete set of right-eigenvectors is given by:

$$\mathbf{r_{0,1}} = \left(\frac{\mathcal{K}}{hW}, v_x, v_y, v_z, 1 - \frac{\mathcal{K}}{hW} \right)^T \tag{66}$$

$$\mathbf{r_{0,2}} = \big(Wv_y, h(\gamma_{xy}+2W^2v_xv_y), h(\gamma_{yy}+2W^2v_yv_y), h(\gamma_{zy}+2W^2v_zv_y), Wv_y(2hW-1)\big)^T \quad (67)$$

$$\mathbf{r_{0,3}} = \big(Wv_z, h(\gamma_{xz}+2W^2v_xv_z), h(\gamma_{yz}+2W^2v_yv_z), h(\gamma_{zz}+2W^2v_zv_z), Wv_z(2hW-1)\big)^T \quad (68)$$

$$\mathbf{r}_{\pm} = (1, hW\mathcal{C}^x_{\pm}, hWv_y, hWv_z, hW\tilde{\mathcal{A}}^x_{\pm}-1)^T \quad (69)$$

(superscript T denotes transpose), where the following auxiliary quantities are used:

$$\mathcal{K} \equiv \frac{\tilde{\kappa}}{\tilde{\kappa}-c_s^2}, \qquad \tilde{\kappa} \equiv \kappa/\rho, \qquad \mathcal{C}^x_{\pm} \equiv v_x - \mathcal{V}^x_{\pm} \quad (70)$$

$$\mathcal{V}^x_{\pm} \equiv \frac{v^x - \Lambda^x_{\pm}}{\gamma^{xx} - v^x\Lambda^x_{\pm}} \qquad \tilde{\mathcal{A}}^x_{\pm} \equiv \frac{\gamma^{xx} - v^xv^x}{\gamma^{xx} - v^x\Lambda^x_{\pm}} \quad (71)$$

$$\Lambda^i_{\pm} \equiv \tilde{\lambda}_{\pm} + \tilde{\beta}^i, \qquad \tilde{\lambda} \equiv \lambda/\alpha, \qquad \tilde{\beta}^i \equiv \beta^i/\alpha \quad (72)$$

Finally, a complete set of left-eigenvectors is given by

$$\mathbf{l}_{0,1} = \frac{W}{\mathcal{K}-1}\,(h-W, Wv^x, Wv^y, Wv^z, -W)^T \quad (73)$$

$$\mathbf{l}_{0,2} = \frac{1}{h\xi}\begin{bmatrix} -\gamma_{zz}v_y + \gamma_{yz}v_z \\ v^x(\gamma_{zz}v_y - \gamma_{yz}v_z) \\ \gamma_{zz}(1-v_xv^x) + \gamma_{xz}v_zv^x \\ -\gamma_{yz}(1-v_xv^x) - \gamma_{xz}v_yv^x \\ -\gamma_{zz}v_y + \gamma_{yz}v_z \end{bmatrix} \quad (74)$$

$$\mathbf{l}_{0,3} = \frac{1}{h\xi}\begin{bmatrix} -\gamma_{yy}v_z + \gamma_{zy}v_y \\ v^x(\gamma_{yy}v_z - \gamma_{zy}v_y) \\ -\gamma_{zy}(1-v_xv^x) - \gamma_{xy}v_zv^x \\ \gamma_{yy}(1-v_xv^x) + \gamma_{xy}v_yv^x \\ -\gamma_{yy}v_z + \gamma_{zy}v_y \end{bmatrix} \quad (75)$$

$$\mathbf{l}_{\mp} = \pm\frac{h^2}{\Delta}\begin{bmatrix} hW\mathcal{V}^x_{\pm}\xi + l^{(5)}_{\mp} \\ \Gamma_{xx}(1-\mathcal{K}\tilde{\mathcal{A}}^x_{\pm}) + (2\mathcal{K}-1)\mathcal{V}^x_{\pm}(W^2v^x\xi - \Gamma_{xx}v^x) \\ \Gamma_{xy}(1-\mathcal{K}\tilde{\mathcal{A}}^x_{\pm}) + (2\mathcal{K}-1)\mathcal{V}^x_{\pm}(W^2v^y\xi - \Gamma_{xy}v^x) \\ \Gamma_{xz}(1-\mathcal{K}\tilde{\mathcal{A}}^x_{\pm}) + (2\mathcal{K}-1)\mathcal{V}^x_{\pm}(W^2v^z\xi - \Gamma_{xz}v^x) \\ (1-\mathcal{K})[-\gamma v^x + \mathcal{V}^x_{\pm}(W^2\xi - \Gamma_{xx})] - \mathcal{K}W^2\mathcal{V}^x_{\pm}\xi \end{bmatrix} \tag{76}$$

where the following relations and auxiliary quantities have been used:

$$1 - \tilde{\mathcal{A}}^x_{\pm} = v^x\mathcal{V}^x_{\pm}, \qquad \tilde{\mathcal{A}}^x_{\pm} - \tilde{\mathcal{A}}^x_{\mp} = v^x(\mathcal{C}^x_{\pm} - \mathcal{C}^x_{\mp}) \tag{77}$$

$$(\mathcal{C}^x_{\pm} - \mathcal{C}^x_{\pm}) + (\tilde{\mathcal{A}}^x_{\mp}\mathcal{V}^x_{\pm} - \tilde{\mathcal{A}}^x_{\pm}\mathcal{V}^x_{\mp}) = 0 \tag{78}$$

$$\Delta \equiv h^3W(\mathcal{K}-1)(\mathcal{C}^x_{+} - \mathcal{C}^x_{-})\xi \qquad \xi \equiv \Gamma_{xx} - \gamma v^x v^x \tag{79}$$

$$\gamma \equiv \det\gamma_{ij} = \gamma_{xx}\Gamma_{xx} + \gamma_{xy}\Gamma_{xy} + \gamma_{xz}\Gamma_{xz}, \qquad \Gamma_{xx} = \gamma_{yy}\gamma_{zz} - \gamma^2_{yz} \tag{80}$$

$$\Gamma_{xx}v_x + \Gamma_{xy}v_y + \Gamma_{xz}v_z = \gamma v^x \tag{81}$$

These two sets of eigenfields reduce to the corresponding ones in the Minkowskian limit [48].

Acknowledgments

It is a pleasure to acknowledge José M. Ibáñez, Ewald Müller and Philippos Papadopoulos for valuable suggestions and a careful reading of the manuscript. I am particularly grateful to Konstantinos Kifonidis, José V. Romero and Wai-Mo Suen for providing some of the movies contained in this paper. This work has been supported in part by a TMR fellowship from the European Union (contract nr. ERBFMBICT971902). The author has made use of NASA's Astrophysics Data System Abstract Service which is gratefully acknowledged.

References

[1] Abrahams, A. M., Cook, G. B., Shapiro, S. L., and Teukolsky, S. A., "Solving Einstein Equations for Rotating Spacetimes: Evolution of Relativistic Star Clusters", *Phys. Rev. D*, **49**, 5153–5164, (1994).

[2] Abramowicz, M., Jaroszynski, M., and Sikora, M., "Relativistic, accreting disks", *Astron. Astrophys.*, **63**, 221–224, (1978).

[3] Alcubierre, M., Allen, G., Brügmann, B., Dramlitsch, Th., Font, J. A., Miller, M., Papadopoulos, P., Seidel, E., Stergioulas, N., Suen, W.-M., Takahashi, R., and Tobias, M., "Towards a Stable Numerical Evolution of Strongly Gravitating Systems in General Relativity: The Conformal Treatments", (1999). In preparation.

[4] Aloy, M. A., Ibáñez, J. M., Martí, and Müller, E., "GENESIS: A high-resolution code for three-dimensional relativistic hydrodynamics", *Astrophys. J. Suppl. Ser.*, **122**, 151–166, (1999). For a related online version see: M. A. Aloy, et al., "GENESIS: A high-resolution code for three-dimensional relativistic hydrodynamics", (March, 1999), http://xxx.lanl.gov/abs/astro-ph/9903352.

[5] Anile, A. M., *Relativistic fluids and magneto-fluids*, (Cambridge University Press, Cambridge, England, 1989).

[6] Anninos, P., "Computational Cosmology: from the Early Universe to the Large Scale Structure", *Living Reviews in Relativity*, **1**, (1998).

[7] Anninos, P., "Plane-symmetric cosmology with relativistic hydrodynamics", *Phys. Rev. D*, **58**, 064010,1–11, (1998).

[8] Arnett, W. D., "Gravitational collapse and weak interactions", *Can. J. Phys.*, **44**, 2553–2594, (1966).

[9] Arnowitt, R., Deser, S., and Misner, C. W., "The Dynamics of General Relativity", in Witten, L., ed., *Gravitation: An Introduction to Current Research*, 227–265, (John Wiley, New York, 1962).

[10] Balbus, S. A., and Hawley, J. A., "Instability, turbulence, and enhanced transport in accretion disks", *Rev. of Mod. Phys.*, **70**, 1–53, (1998).

[11] Balsara, D., "Riemann solver for relativistic hydrodynamics", *J. Comput. Phys.*, **114**, 284–297, (1994).

[12] Banyuls, F., Font, J. A., Ibáñez, J. M., Martí, J. M., and Miralles, J. A., "Numerical 3+1 General Relativistic Hydrodynamics: A Local Characteristic Approach", *Astrophys. J.*, **476**, 221–231, (1997).

[13] Bardeen, J. M., and Piran, T., "General relativistic axisymmetric rotating systems: coordinates and equations", *Phys. Rep.*, **96**, No. 4, 205–250, (1983).

[14] Bardeen, J. M., and Press, W. H., "Radiation fields in the Schwarzschild background", *J. Math. Phys.*, **14**, 7–19, (1972).

[15] Baron, E., Cooperstein, J., and Kahana, S., "Type-II Supernovae in $12M_\odot$ and $15M_\odot$ stars: the equation of state and general relativity", *Phys. Rev. Lett.*, **55**, 126–129, (1985).

[16] Baumgarte, T. W., Hughes, S. A., and Shapiro, S. L., "Evolving Einstein's field equations with matter: The "hydro without hydro" test", (1999). For a related online version see: T. W. Baumgarte, et al., "Evolving Einstein's field equations with matter: The "hydro without hydro" test", (February, 1999), http://xxx.lanl.gov/abs/gr-qc/9902024. Submitted to Phys. Rev. D.

[17] Baumgarte, T. W., and Shapiro, S. L., "On the numerical integration of Einstein's field equations", *Phys. Rev. D*, **59**, 024007, (1999). For a related online version see: T. W. Baumgarte, et al., "On the numerical integration of Einstein's field equations", (October, 1998), http://xxx.lanl.gov/abs/gr-qc/9810065.

[18] Baumgarte, T. W., Shapiro, S. L., and Teukolsky, S. A., "Computing supernova collapse to neutron stars and black holes", *Astrophys. J.*, **443**, 717–734, (1995).

[19] Benensohn, J. S., Lamb, D. Q., and Taam, R. E., "Hydrodynamical studies of wind accretion onto compact objects: Two-dimensional calculations", *Astrophys. J.*, **478**, 723–733, (1997). For a related online version see: J. S. Benensohn, et al., "Hydrodynamical studies of wind accretion onto compact objects: Two-dimensional calculations", (October, 1996), http://xxx.lanl.gov/abs/astro-ph/9610245.

[20] Bethe, H. A., "Supernova mechanisms", *Rev. Mod. Phys.*, **62**, 801–866, (1990).

[21] Bethe, H. A., and Wilson, J. R., "Revival of a stalled supernova shock by neutrino heating", *Astrophys. J.*, **295**, 14–23, (1985).

[22] Bishop, N. T., Gómez, R., Lehner, L., Maharaj, M., and Winicour, J., "The incorporation of matter into characteristic numerical relativity", *Phys. Rev. D*, **60**, 024005, (1999). For a related online version see: N. T. Bishop, et al., "The incorporation of matter into characteristic numerical relativity", (January, 1999), http://xxx.lanl.gov/abs/gr-qc/9901056.

[23] Blandford, R. D., "Relativistic accretion", in *Astrophysical discs*, ASP Conference Series, (1999). For a related online version see: R. D. Blandford, "Relativistic accretion", (January, 1999), http://xxx.lanl.gov/abs/astro-ph/9902001. in press.

[24] Blandford, R. D., and Znajek, R. L., "Electromagnetic extraction of energy from Kerr black holes", *Mon. Not. R. Astron. Soc.*, **179**, 433–456, (1977).

[25] Bona, C., Ibáñez, J. M., Martí, J. M., and Massó, J., "Gravitation and General Relativity: rotating bodies and other topics", volume 423 of *Lecture Notes in Physics*, (Springer-Verlag, New York, 1993).

[26] Bona, C., and Massó, J., "Einstein's evolution equations as a system of balance laws", *Phys. Rev. D*, **40**, 1022–1026, (1989).

[27] Bona, C., Massó, J., Seidel, E., and Stela, J., "A new formalism for numerical relativity", *Phys. Rev. Lett.*, **75**, 600–603, (1995). For a related online version see: C. Bona, et al., "New formalism for numerical relativity", (December, 1994), http://xxx.lanl.gov/abs/gr-qc/9412071.

[28] Bonazzola, S., Gourgoulhon, and Marck, J.-A., "Spectral methods in general relativistic astrophysics", *J. Comput. Appl. Math.*, (1999). For a related online version see: S. Bonazzola, et al., "Spectral methods in general relativistic astrophysics", (November, 1998), http://xxx.lanl.gov/abs/gr-qc/9811089. in press.

[29] Bonazzola, S., and Marck, J.-A., "Efficiency of gravitational radiation from axisymmetric and 3D stellar collapse. I. Polytropic case", *Astron. Astrophys.*, **267**, 623–633, (1993).

[30] Bondi, H., "On spherically symmetric accretion", *Mon. Not. R. Astron. Soc.*, **112**, 195–204, (1952).

[31] Bondi, H., and Hoyle, F., "On the mechanism of accretion by stars", *Mon. Not. R. Astron. Soc.*, **104**, 273–282, (1944).

[32] Bondi, H., van der Burg, M. J. G., and Metzner, A. W. K., "Gravitational waves in general relativity. VII. Waves from axi-symmetric isolated systems", *Proc. R. Soc. London*, **Sect. A 269**, 21–52, (1962).

[33] Boris, J. P., and Book, D. L., "Flux corrected transport I, SHASTA, a fluid transport algorithm that works", *J. Comput. Phys.*, **11**, 38–69, (1973).

[34] Bromley, B. C., Miller, W.A., and Pariev, V. I., "The inner edge of the accretion disk around a supermassive black hole", *Nature*, **391**, 54–56, (1998).

[35] Bruenn, S. W., "Stellar core collapse: numerical model and infall epoch", *Astrophys. J. Suppl. Ser.*, **58**, 771–841, (1985).

[36] Bruenn, S. W., "The prompt-shock supernova mechanism. I - The effect of the free-proton mass fraction and the neutrino transport algorithm", *Astrophys. J*, **340**, 955–965, (1989).

[37] Bruenn, S. W., in Guidry, M. W., and Strayer, M. R., eds., *Nuclear physics in the universe*, (IOP, Bristol, 1993).

[38] Canuto, C, Hussaini, M. Y., Quarteroni, A., and Zang, T. A., *Spectral methods in fluid dynamics*, (Springer-Verlag, Berlin, 1988).

[39] Centrella, J., and Wilson, J. R., "Planar numerical cosmology. I. The differential equations", *Astrophys. J.*, **273**, 428–435, (1983).

[40] Centrella, J., and Wilson, J. R., "Planar numerical cosmology. II. The difference equations and numerical tests", *Astrophys. J. Suppl. Ser.*, **54**, 229–249, (1984).

[41] Chandrasekhar, S., *The mathematical theory of black holes*, (Oxford University Press, New York, 1983).

[42] Choptuik, M. W., "Universality and scaling in gravitational collapse of a massless scalar field", *Phys. Rev. Lett.*, **70**, 9–12, (1993).

[43] Chow, E., and Monaghan, J. J., "Ultrarelativistic SPH", *J. Comput. Phys.*, **134**, 296–305, (1997).

[44] Colella, P., and Woodward, P. R., "The piecewise parabolic method (PPM) for gas-dynamical simulations", *J. Comput. Phys.*, **54**, 174–201, (1984).

[45] Colgate, S. A., "Hot bubbles drive explosions", *Nature*, **341**, 489–490, (1989).

[46] Colgate, S. A., and White, R. H., "The hydrodynamic behaviour of supernovae explosions", *Astrophys. J.*, **143**, 626–681, (1966).

[47] Dolezal, A., and Wong, S. S. M., "Relativistic hydrodynamics and Essentially Non-Oscillatory shock capturing schemes", *J. Comput. Phys.*, **120**, 266–277, (1995).

[48] Donat, R., Font, J. A., Ibáñez, J. M., and Marquina, A., "A Flux-Split Algorithm applied to Relativistic Flows", *J. Comput. Phys.*, **146**, 58–81, (1998).

[49] Donat, R., and Marquina, A., "Capturing shock reflections: an improved flux formula", *J. Comput. Phys.*, **125**, 42–58, (1996).

[50] Dubal, M. R., d'Inverno, R. A., and Vickers, J. A., "Combining Cauchy and characteristic codes. V. CCM for a spherical spacetime containing a perfect fluid", *Phys. Rev. D*, **58**, 044019, (1998).

[51] Dykema, P. G., *Numerical simulation of axisymmetric gravitational collapse*, PhD thesis, (University of Texas at Austin, 1980).

[52] Eckart, C., "The thermodynamics of irreversible processes, III: Relativistic theory of the simple fluid", *Phys. Rev.*, **58**, 919–924, (1940).

[53] Einfeldt, B., "On Godunov-type methods for gas dynamics", *SIAM J. Num. Anal.*, **25**, 294–318, (1988).

[54] Eulderink, F., *Numerical relativistic hydrodynamics*, PhD thesis, (Rijksuniversitet Leiden, 1993).

[55] Eulderink, F., and Mellema, G., "Special relativistic jet collimation by inertial confinement", *Astron. Astrophys.*, **284**, 654–662, (1994).

[56] Eulderink, F., and Mellema, G., "General relativistic hydrodynamics with a Roe solver", *Astron. Astrophys. Suppl. Ser.*, **110**, 587–623, (1995). For a related online version see: F. Eulderink, et al., "General relativistic hydrodynamics with a Roe solver", (November, 1994), http://xxx.lanl.gov/abs/astro-ph/9411056.

[57] Evans, C., "An Approach for Calculating Axisymmetric Gravitational Collapse", in Centrella, J., ed., *Dynamical Spacetimes and Numerical Relativity*, 3–39, (Cambridge University Press, Cambridge, England, 1986).

[58] Evans, C., and Hawley, J. F., "Simulation of magnetohydrodynamic flows: a constrained transport method", *Astrophys. J.*, **332**, 659–677, (1988).

[59] Evans, C. R., Smarr, L. L., and Wilson, J. R., "Numerical relativistic gravitational collapse with spatial time slices", in Norman, M. L., and Winkler, K-H. A., eds., *Astrophysical Radiation Hydrodynamics*, 491–529. Reidel Publishing Company, (1986).

[60] Falle, S. A. E. G., and Komissarov, S. S., "An upwind numerical scheme for relativistic hydrodynamics with a general equation of state", *Mon. Not. Roy. Astron. Soc.*, **278**, 586–602, (1996).

[61] Font, J. A., Goodale, T., Miller, M., Seidel, E., Stergioulas, N., , Suen, W.-M., and Tobias, M., "Three-dimensional numerical general relativistic hydrodynamics: Dynamical evolutions of neutron stars and long-term stabilities", (1999). In preparation.

[62] Font, J. A., and Ibáñez, J. M., "Non-axisymmetric Relativistic Bondi-Hoyle Accretion onto a Schwarzschild Black Hole", *Mon. Not. R. Astron. Soc.*, **298**, 835–846, (1998). For a related online version see: J. A. Font, et al., "Non-axisymmetric Relativistic Bondi-Hoyle Accretion onto a Schwarzschild Black Hole", (April, 1998), http://xxx.lanl.gov/abs/astro-ph/9804254.

[63] Font, J. A., and Ibáñez, J. M., "A Numerical Study of Relativistic Bondi-Hoyle Accretion onto a Moving Black Hole: Axisymmetric Computations in a Schwarzschild Background", *Astrophys. J.*, **494**, 297–316, (1998).

[64] Font, J. A., Ibáñez, J. M., Martí, J. M., and Marquina, A., "Multidimensional relativistic hydrodynamics: characteristic fields and modern high-resolution shock-capturing schemes", *Astron. Astrophys.*, **282**, 304–314, (1994).

[65] Font, J. A., Ibáñez, J. M., and Papadopoulos, P., "A horizon-adapted approach to the study of relativistic accretion flows onto rotating black holes", *Astrophys. J. Lett.*, **507**, L67–L70, (1998). For a related online version see: J. A. Font, et al., "A horizon-adapted approach to the study of relativistic accretion flows onto rotating black holes", (May, 1998), http://xxx.lanl.gov/abs/astro-ph/9805269.

[66] Font, J. A., Ibáñez, J. M., and Papadopoulos, P., "Non-axisymmetric Relativistic Bondi-Hoyle Accretion onto a Kerr Black Hole", *Mon. Not. R. Astron. Soc.*, **305**, 920–936, (1999). For a related online version see: J. A. Font, et al., "Non-axisymmetric Relativistic Bondi-Hoyle Accretion onto a Kerr Black Hole", (October, 1998), http://xxx.lanl.gov/abs/astro-ph/9810344.

[67] Font, J. A., Miller, M., Suen, W.-M., and Tobias, M., "Three Dimensional Numerical General Relativistic Hydrodynamics: Formulations, Methods and Code Tests", (1999). For a related online version see: J. A. Font, et al., "Three Dimensional Numerical General Relativistic Hydrodynamics: Formulations, Methods and Code Tests", (November, 1998), http://xxx.lanl.gov/abs/astro-ph/9811015. submitted to Phys. Rev. D.

[68] Frank, J., King, A., and Raine, D., *Accretion power in astrophysics*, (Cambridge University Press, Cambridge, England, 1992).

[69] Friedrichs, K. O., "On the laws of relativistic electromagneto-fluid dynamics", *Commun. Pure Appl. Math.*, **27**, 749–808, (1974).

[70] Fryxell, B. A., Müller, E., and Arnett, W. D., *Max-Planck-Institut für Astrophysik preprint*, **449**, (1989).

[71] Gingold, R. A., and Monaghan, J. J., "Smoothed particle hydrodynamics - Theory and application to non-spherical stars", *Mon. Not. R. Astron. Soc.*, **181**, 375–389, (1977).

[72] Glaister, P., "An approximate linearised Riemann solver for the Euler equations for real gases", *J. Comput. Phys.*, **74**, 382–408, (1988).

[73] Glendening, N. K., *Compact stars. Nuclear physics, particle physics and general relativity*, Astronomy and astrophysics library, (Springer-Verlag, Berlin, 1997).

[74] Godunov, S. K., "A finite difference method for the numerical computation and discontinuous solutions of the equations of fluid dynamics", *Mat. Sb.*, **47**, 271, (1959). in Russian.

[75] Gómez, R., Papadopoulos, P., and Winicour, J., "Null cone evolution of axisymmetric vacuum space-times", *J. Math. Phys.*, **35**, 4184–4204, (1994).

[76] Gottlieb, D., and Orszag, S. A., *Numerical analysis of spectral methods: theory and applications*, (Society for Industrial and Applied Mathematics, Philadelphia, 1977).

[77] Gourgoulhon, E., "Simple equations for general relativistic hydrodynamics in spherical symmetry applied to neutron star collapse", *Astron. Astrophys.*, **252**, 651–663, (1991).

[78] Harten, A., "On a class of high resolution total-variation stable finite difference schemes", *SIAM J. Numer. Anal.*, **21**, 1–23, (1984).

[79] Harten, A., Engquist, B., Osher, S., and Chakrabarthy, S. R., "Uniformly high order accurate essentially non-oscillatory schemes, III", *J. Comp. Phys.*, **71**, 231–303, (1987).

[80] Harten, A., Lax, P. D., and van Leer, B., "On upstream differencing and Godunov-type schemes for hyperbolic conservation laws", *SIAM Review*, **25**, 35–61, (1983).

[81] Haugan, M. P., Shapiro, S. L., and Wasserman, I., "The suppression of gravitational radiation from finite-size stars falling into black holes", *Astrophys. J.*, **257**, 283–290, (1982).

[82] Hawley, J. F., "General relativistic hydrodynamics near black holes", in Centrella, J., ed., *Dynamical Spacetimes and Numerical Relativity*, 101–122, (Cambridge University Press, Cambridge, England, 1986).

[83] Hawley, J. F., "Three-dimensional simulations of black hole tori", *Astrophys. J.*, **381**, 496–507, (1991).

[84] Hawley, J. F., Smarr, L. L., and Wilson, J. R., "A numerical study of nonspherical black hole accretion. I. Equations and test problems", *Astrophys. J.*, **277**, 296–311, (1984).

[85] Hawley, J. F., Smarr, L. L., and Wilson, J. R., "A numerical study of nonspherical black hole accretion. II. Finite differencing and code calibration", *Astrophys. J. Suppl. Ser.*, **55**, 211–246, (1984).

[86] Hernández, W. C., and Misner, C. W., "Observer time as a coordinate in relativistic spherical hydrodynamics", *Astrophys. J.*, **143**, 452–464, (1966).

[87] Hoyle, F., and Lyttleton, R. A., *Proc. Cambridge Phil. Soc.*, **35**, 405, (1939).

[88] Ibáñez, J. M., in Chinea, F. J., and González-Romero, L. M., eds., *Lecture Notes in Physics, Vol. 423, Rotating objects and relativistic physics*, 149, (Springer-Verlag, Berlin, 1993).

[89] Ibáñez, J. M., Aloy, M. A., Font, J. A., Martí, J. M., Miralles, J. A., and Pons, J. A., "Riemann solvers in general relativistic hydrodynamics", in Toro, E.F., ed., *Godunov methods: theory and applications*, (1999).

[90] Ibáñez, J. M., and Martí, J. M., "Riemann solvers in relativistic astrophysics", *J. Comput. Appl. Math.*, **109**, 173–211, (1999).

[91] Ibáñez, J. M., Martí, J. M., Miralles, J. A., and Romero, J. V., in d'Inverno, R., ed., *Approaches to numerical relativity*, 223, (Cambridge University Press, Cambridge, England, 1992).

[92] Igumenshchev, I. V., and Belodorov, A. M., "Numerical simulations of thick disc accretion on to a rotating black hole", *Mon. Not. R. Astron. Soc.*, **284**, 767–772, (1997).

[93] Isaacson, R. A., Welling, J. S., and Winicour, J., "Null cone computation of gravitational radiation", *J. Math. Phys.*, **24**, 1824–1834, (1983).

[94] Israel, W., and Stewart, J. M., "Transient relativistic thermodynamics and kinetic theory", *Ann. Phys.*, **118**, 341–372, (1979).

[95] Janka, H.-Th., Zwerger, Th., and Mönchmeyer, R, "Does artificial viscosity destroy prompt type-II supernova explosions?", *Astron. Astrophys.*, **268**, 360–368, (1993).

[96] Kheyfets, A., Miller, W. A., and Zurek, W. H., "Covariant smoothed particle hydrodynamics on a curved background", *Phys. Rev. D*, **41**, 451–454, (1990).

[97] Kifonidis, K., Plewa, T, Janka, H.-Th., and Müller, E., "Nucleosynthesis and clump formation in a core collapse supernova", *Astrophys. J. Lett.*, (1999). For a related online version see: K. Kifonidis, et al., "Nucleosynthesis and clump formation in a core collapse supernova", (November, 1999), http://xxx.lanl.gov/abs/astro-ph/9911183. Submitted.

[98] Koide, S., Shibata, K., and Kudoh, T., "General relativistic magnetohydrodynamic simulations of jets from black hole accretion disks: Two-component jets driven by nonsteady accretion of magnetized disks", *Astrophys. J.*, **495**, L63–L66, (1998).

[99] Komissarov, S. S., "A Godunov-type scheme for relativistic magnetohydrodynamics", *Mon. Not. Roy. Astron. Soc.*, **303**, 343–366, (1999).

[100] Kormendy, J., and Richstone, D., "Inward Bound—The Search For Supermassive Black Holes In Galactic Nuclei", *Ann. Rev. Astron. Astrophys.*, **33**, 581–624, (1995).

[101] Laguna, P., Miller, W. A., and Zurek, W. H., "Smoothed particle hydrodynamics near a black hole", *Astrophys. J.*, **404**, 678–685, (1993).

[102] Laguna, P., Miller, W. A., Zurek, W. H., and Davies, M. B., "Tidal disruptions by supermassive black holes: Hydrodynamic evolution of stars on a Schwarzschild background", *Astrophys. J.*, **410**, L83–L86, (1993).

[103] Lattimer, J. M., and Swesty, F. D., "A generalized equation of state for hot, dense matter", *Nucl. Phys. A*, **535**, 331–376, (1991).

[104] LeVeque, R. J., *Numerical Methods for Conservation Laws*, (Birkhauser Verlag, Basel, 1992).

[105] LeVeque, R. J., "Nonlinear conservation laws and finite volume methods for astrophysical fluid flow", in Steiner, O., and Gautschy, A., eds., *Computational methods for astrophysical fluid flow*, 1–159, (Springer-Verlag, Berlin, 1998).

[106] Liu, I. S., Müller, I., and Ruggeri, T., "Relativistic thermodynamics of gases", *Ann. Phys.*, **169**, 191–219, (1986).

[107] Lucy, L. B., "A numerical approach to the testing of the fission hypothesis", *Astronom. J.*, **82**, 1013–1024, (1977).

[108] Mann, P. J., "A relativistic smoothed particle hydrodynamics method tested with the shock tube", *Comput. Phys. Comm.*, **67**, 245–260, (1991).

[109] Marck, J.-A., Lioure, A., and Bonazzola, S., "Numerical study of the tidal interaction of a star and a massive black hole", *Astron. Astrophys.*, **306**, 666–674, (1996). For a related online version see: J.-A. Marck, et al., "Numerical study of the tidal interaction of a star and a massive black hole", (May, 1995), http://xxx.lanl.gov/abs/astro-ph/9505027.

[110] Martí, J. M., *Hidrodinámica relativista numérica: aplicaciones al colapso estelar*, PhD thesis, (Universidad de Valencia, 1991). In Spanish.

[111] Martí, J. M., Ibáñez, J. M., and Miralles, J. A., "Godunov-type methods for stellar collapse", *Astron. Astrophys.*, **235**, 535–542, (1990).

[112] Martí, J. M., Ibáñez, J. M., and Miralles, J. A., "Numerical relativistic hydrodynamics: local characteristic approach", *Phys. Rev. D*, **43**, 3794–3801, (1991).

[113] Martí, J. M., and Müller, E., "The analytical solution of the Riemann problem in relativistic hydrodynamics", *J. Fluid. Mech.*, **258**, 317–333, (1994).

[114] Martí, J. M., and Müller, E., "Extension of the piecewise parabolic method to one-dimensional relativistic hydrodynamics", *J. Comput. Phys.*, **123**, 1–14, (1996).

[115] Martí, J. M., and Müller, E., "Numerical hydrodynamics in special relativity", *Living Reviews in Relativity*, **1**, (1999). For a related online version see: J. M. Martí, et al., "Numerical hydrodynamics in special relativity", (June, 1999), http://xxx.lanl.gov/abs/gr-qc/9906333.

[116] Martí, J. M., Müller, E., Font, J. A., Ibáñez, J. M., and Marquina, A., "Morphology and dynamics of relativistic jets", *Astrophys. J.*, **479**, 151–163, (1997).

[117] Mathews, G. J., Marronetti, P., and Wilson, J. R., "Relativistic Hydrodynamics in Close Binary Systems: Analysis of Neutron-Star Collapse", *Phys. Rev. D*, **58**, 043003, (1998). For a related online version see: G. J. Mathews, et al., "Relativistic Hydrodynamics in Close Binary Systems: Analysis of Neutron-Star Collapse", (October, 1997), http://xxx.lanl.gov/abs/gr-qc/9710140.

[118] May, M. M., and White, R. H., "Hydrodynamic calculations of general relativistic collapse", *Phys. Rev. D*, **141**, 1232–1241, (1966).

[119] May, M. M., and White, R. H., "Stellar dynamics and gravitational collapse", *Meth. Computat. Phys.*, **7**, 219–258, (1967).

[120] Mayle, R., Wilson, J. R., and Schramm, D. N., "Neutrinos from gravitational collapse", *Astrophys. J.*, **318**, 288–306, (1987).

[121] McAbee, T. L., and Wilson, J. R., "Mean-field pion calculations of heavy-ion collisions at Bevalac energies", *Nucl. Phys. A*, **576**, 626–638, (1994).

[122] Mezzacappa, A., and Matzner, R. A., "Computer simulation of time-dependent, spherically symmetric spacetimes containing radiating fluids - Formalism and code tests", *Astrophys. J.*, **343**, 853–873, (1989).

[123] Michel, F. C., "Accretion of matter by condensed objects", *Astrophys. Spa. Sci.*, **15**, 153–160, (1972).

[124] Mihalas, D., and Mihalas, B., *Foundations of radiation hydrodynamics*, (Oxford University Press, Oxford, England, 1984).

[125] Miller, J. C., and Motta, S., "Computations of spherical gravitational collapse using null slicing", *Class. Quant. Grav.*, **6**, 185–193, (1989).

[126] Miller, M., Suen, W.-M., and Tobias, M., "The Shapiro Conjecture: Prompt or Delayed Collapse in the head-on collision of neutron stars?", (1999). For a related online version see: M. Miller, et al., "The Shapiro Conjecture: Prompt or Delayed Collapse in the head-on collision of neutron stars?", (April, 1999), http://xxx.lanl.gov/abs/gr-qc/9904041. Submitted to Phys. Rev. Lett.

[127] Miralles, J. A., Ibáñez, J. M., Martí, J. M., and Pérez, A., "Incompressibility of hot nuclear matter, general relativistic stellar collapse and shock propagation", *Astron. Astrophys. Suppl. Ser.*, **90**, 283–299, (1991).

[128] Misner, C. W., and Sharp, D. H., "Relativistic equations for adiabatic, spherically symmetric, gravitational collapse", *Phys. Rev.*, **136**, 571–576, (1964).

[129] Misner, C. W., Thorne, K. S., and Wheeler, J. A., *Gravitation*, (W. H. Freeman, San Francisco, 1973).

[130] Monaghan, J. J., "Smoothed particle hydrodynamics", *Ann. Rev. Astron. Astrophys.*, **30**, 543–574, (1992).

[131] Müller, E, "Gravitational radiation from collapsing rotating stellar cores", *Astron. Astrophys.*, **114**, 53–59, (1982).

[132] Müller, E, "Simulation of astrophysical fluid flow", in Steiner, O., and Gautschy, A., eds., *Computational methods for astrophysical fluid flow*, 343–494, (Springer-Verlag, Berlin, 1998).

[133] Müller, I, "Speeds of propagation in classical and relativistic extended thermodynamics", *Living Reviews in Relativity*, **2**, (1999).

[134] Nakamura, T., "General relativistic collapse of axially symmetric stars leading to the formation of rotating black holes", *Prog. Theor. Phys.*, **65**, 1876–1890, (1981).

[135] Nakamura, T., Maeda, K., Miyama, S., and Sasaki, M., "General relativistic collapse of an axially symmetric star", *Prog. Theor. Phys.*, **63**, 1229–1244, (1980).

[136] Nakamura, T., and Oohara, K., "A Way to 3D Numerical Relativity - Coalescing Binary Neutron Stars", in *Numerical astrophysics*, (1998). For a related online version see: T. Nakamura, et al., "A Way to 3D Numerical Relativity - Coalescing Binary Neutron Stars", (December, 1998), http://xxx.lanl.gov/abs/gr-qc/9812054.

[137] Nakamura, T., and Sasaki, M., "Is collapse of a deformed star always effectual for gravitational radiation?", *Phys. Letters*, **106 B**, 69–72, (1981).

[138] Nakamura, T., and Sato, H., "General relativistic collapse of non-rotating, axisymmetric stars", *Prog. Theor. Phys.*, **67**, 1396–1405, (1982).

[139] Narayan, R., Paczyński, B., and Piran, T., "Gamma-ray bursts as the death throes of massive binary stars", *Astrophys. J.*, **395**, L83–L86, (1992).

[140] Neilsen, D. W., and Choptuik, M. W., "Critical phenomena in perfect fluids", *Class. Quant. Grav.*, (1999). For a related online version see: D. W. Neilsen, et al., "Critical phenomena in perfect fluids", (December, 1998), http://xxx.lanl.gov/abs/gr-qc/9812053. Submitted.

[141] Neilsen, D. W., and Choptuik, M. W., "Ultrarelativistic fluid dynamics", *Class. Quant. Grav.*, (1999). For a related online version see: D. W. Neilsen, et al., "Ultrarelativistic fluid dynamics", (April, 1999), http://xxx.lanl.gov/abs/gr-qc/9804052. Submitted.

[142] Noh, W. F., "Errors for calculations of strong shocks using an artificial viscosity and an artificial heat flux", *J. Comput. Phys.*, **72**, 78–120, (1987).

[143] Norman, M. L., and Winkler, K-H. A., "Why ultrarelativistic numerical hydrodynamics is difficult?", in Norman, M. L., and Winkler, K-H. A., eds., *Astrophysical Radiation Hydrodynamics*, 449–475. Reidel Publishing Company, (1986).

[144] Novak, J., "Spherical neutron star collapse in tensor-scalar theory of gravity", *Phys. Rev. D*, **57**, 4789–4801, (1998). For a related online version see: J. Novak, "Spherical neutron star collapse toward a black hole in tensor-scalar theory of gravity", (July, 1997), http://xxx.lanl.gov/abs/gr-qc/9707041.

[145] Oohara, K., and Nakamura, T., "Gravitational radiation from a particle scattered by a non-rotating black hole", *Phys. Lett. A*, **98**, 407–410, (1983).

[146] Oohara, K.-I., and Nakamura, T., "Coalescence of Binary Neutron Stars", in Lasota, Jean-Pierre, and Marck, Jean-Alain, eds., *Relativistic Gravitation and Gravitational Radiation*, (Cambridge University Press, Cambridge, England, 1997). For a related online version see: K.-I. Oohara, et al., "Coalescence of Binary Neutron Stars", (June, 1996), http://xxx.lanl.gov/abs/astro-ph/9606179.

[147] Paczyński, B., "Gamma-ray bursters at cosmological distances", *Astrophys. J.*, **308**, L43–L46, (1986).

[148] Paczyński, B., "Are gamma-ray bursts in star-forming regions?", *Astrophys. J.*, **494**, L45–L48, (1998).

[149] Paczyński, B., and Wiita, P. J., "Thick accretion disks and supercritical luminosities", *Astron. Astrophys.*, **88**, 23–31, (1980).

[150] Papadopoulos, P., and Font, J. A., "Relativistic Hydrodynamics around Black Holes and Horizon Adapted Coordinate Systems", *Phys. Rev. D*, **58**, 024005,1–9, (1998). For a related online version see: P. Papadopoulos, et al., "Relativistic Hydrodynamics around Black Holes and Horizon Adapted Coordinate Systems", (March, 1998), http://xxx.lanl.gov/abs/gr-qc/9803087.

[151] Papadopoulos, P., and Font, J. A., "Matter Flows around Black Holes and Gravitational Radiation", *Phys. Rev. D*, **59**, 044014,1–17, (1999). For a related online version see: P. Papadopoulos, et al., "Matter Flows around Black Holes and Gravitational Radiation", (August, 1998), http://xxx.lanl.gov/abs/gr-qc/9808054.

[152] Papadopoulos, P., and Font, J. A., "Relativistic hydrodynamics on spacelike and null surfaces: Formalism and computations of spherically symmetric spacetimes", *Phys. Rev. D*, (1999). For a related online version see: P. Papadopoulos, et al., "Relativistic hydrodynamics on spacelike and null surfaces: Formalism and computations of spherically symmetric spacetimes", (February, 1999), http://xxx.lanl.gov/abs/gr-qc/9902018. In press.

[153] Papaloizou, J. C. B., and Pringle, J. E., "The dynamical stability of differentially rotating discs with constant specific angular momentum", *Mon. Not. R. Astron. Soc.*, **208**, 721–750, (1984).

[154] Peitz, J., and Appl, S., "Dissipative fluid dynamics in the 3+1 formalism", *Class. Quantum Grav.*, **16**, 979–989, (1999).

[155] Penrose, R., "Gravitational collapse: The role of general relativity", *Riv. Nouvo Cimento*, **1**, 252–276, (1969).

[156] Petrich, L. I., Shapiro, S. L., Stark, R. F., and Teukolsky, S. A., "Accretion onto a moving black hole: a fully relativistic treatment", *Astrophys. J.*, **336**, 313–349, (1989).

[157] Petrich, L. I., Shapiro, S. L., and Wasserman, I., "Gravitational radiation from nonspherical infall into black holes. II. A catalog of "exact" waveforms", *Astrophys. J. Suppl. Ser.*, **58**, 297–320, (1985).

[158] Piran, T., and Stark, R. F., "Numerical relativity, rotating gravitational collapse and gravitational radiation", in Centrella, J., ed., *Dynamical Spacetimes and Numerical Relativity*, 40–73, (Cambridge University Press, Cambridge, England, 1986).

[159] Pons, J. A., Font, J. A., Ibáñez, J. M., Martí, J. M., and Miralles, J. A., "General Relativistic Hydrodynamics with Special Relativistic Riemann Solvers", *Astron. Astrophys.*, **339**, 629–637, (1998). For a related online version see: J. A. Pons, et al., "General Relativistic Hydrodynamics with Special Relativistic Riemann Solvers", (July, 1998), http://xxx.lanl.gov/abs/astro-ph/9807215.

[160] Popham, R., Woosley, S. E., and Fryer, C., "Hyper-accreting black holes and gamma-ray bursts", *Astrophys. J.*, **518**, 356–374, (1998). For a related online version see: R. Popham, et al., "Hyper-accreting black holes and gamma-ray bursts", (July, 1998), http://xxx.lanl.gov/abs/astro-ph/9807028.

[161] Rasio, F. A., and Shapiro, S. L., "Coalescing binary neutron stars", *Class. Quantum Grav.*, **16**, R1–R29, (1999). For a related online version see: F. A. Rasio, et al., "Coalescing binary neutron stars", (February, 1999), http://xxx.lanl.gov/abs/gr-qc/9902019.

[162] Rees, M. J., Begelman, M. C., Blandford, R. D., and Phinney, E. S., "Ion-supported tori and the origin of radio jets", *Nature*, **295**, 17–21, (1982).

[163] Rezzolla, L., and Miller, J. C., "Relativistic radiative transfer for spherical flows", *Class. Quantum Grav.*, **11**, 1815–1832, (1994).

[164] Roe, P. L., "Approximate Riemann solvers, parameter vectors and difference schemes", *J. Comput. Phys.*, **43**, 357–372, (1981).

[165] Romero, J. V., Ibánez, J. M., Martí, J. M., and Miralles, J. A., "A new spherically symmetric general relativistic hydrodynamical code", *Astrophys. J.*, **462**, 839–854, (1996). For a related online version see: J. V. Romero, et al., "A new spherically symmetric general relativistic hydrodynamical code", (September, 1995), http://xxx.lanl.gov/abs/astro-ph/9509121.

[166] Ruffert, M., and Arnett, D., "Three-dimensional hydrodynamic Bondi-Hoyle accretion. 2: Homogeneous medium at Mach 3 with gamma = 5/3", *Astrophys. J.*, **427**, 351–376, (1994).

[167] Ruffert, M., and Janka, H.-T., "Colliding neutron stars. Gravitational waves, neutrino emission, and gamma-ray bursts", *Astron. Astrophys.*, **338**, 535–555, (1998). For a related online version see: M. Ruffert, et al., "Colliding neutron stars — Gravitational waves, neutrino emission, and gamma-ray bursts", (April, 1998), http://xxx.lanl.gov/abs/astro-ph/9804132.

[168] Sachs, R. K., "Gravitational waves in general relativity. VIII. Waves in asymptotically flat space-time", *Proc. R. Soc. London*, **Sect. A 270**, 103–126, (1962).

[169] Schinder, P. J., "General relativistic implicit radiation hydrodynamics in polar sliced spacetime", in C. R. Evans, L. S. Finn, and Hobill, D. W., eds., *Frontiers in numerical relativity*, 163–170, (Cambridge University Press, Cambridge, England, 1989).

[170] Schinder, P. J., Bludmann, S. A., and Piran, T., "General relativistic implicit hydrodynamics in polar sliced spacetime", *Phys. Rev. D*, **37**, 2722–2731, (1988).

[171] Schneider, V., Katscher, V., Rischke, D. H., Waldhauser, B., Marhun, J. A., and Munz, C.-D., "New algorithms for ultra-relativistic numerical hydrodynamics", *J. Comput. Phys.*, **105**, 92–107, (1993).

[172] Seidel, E., and Moore, T., "Gravitational radiation from realistic relativistic stars: Odd-parity fluid perturbations", *Phys. Rev. D*, **35**, 2287–2296, (1987).

[173] Seidel, E., and Moore, T., "Gravitational radiation from perturbations of stellar core collapse models", in C. R. Evans, L. S. Finn, and Hobill, D. W., eds., *Frontiers in numerical relativity*, 146–162, (Cambridge University Press, Cambridge, England, 1989).

[174] Seidel, E., Myra, E. S., and Moore, T., "Gravitational radiation from type II supernovae - The effect of the high-density equation of state", *Phys. Rev. D*, **38**, 2349–2356, (1988).

[175] Shapiro, S. L., and Teukolsky, S. A., "Gravitational collapse to neutron stars and black holes: computer generation of spherical spacetimes", *Astrophys. J.*, **235**, 199–215, (1980).

[176] Shapiro, S. L., and Teukolsky, S. A., "The collapse of dense star clusters to supermassive black holes - The origin of quasars and AGNs", *Astrophys. J.*, **292**, L41–L44, (1985).

[177] Shapiro, S. L., and Teukolsky, S. A., "Computational relativity in two and three dimensions", in C. R. Evans, L. S. Finn, and Hobill, D. W., eds., *Frontiers in numerical relativity*, 18–26, (Cambridge University Press, Cambridge, England, 1989).

[178] Shapiro, S. L., and Teukolsky, S. A., "Formation of naked singularities: the violation of cosmic censorship", *Phys. Rev. Lett.*, **66**, 994–997, (1991).

[179] Shapiro, S. L., and Teukolsky, S. A., "Gravitational collapse of rotating spheroids and the formation of naked singularities", *Phys. Rev. D*, **45**, 2006–2012, (1992).

[180] Shapiro, S. L., and Wasserman, I., "Gravitational radiation from non-spherical infall into black holes", *Astrophys. J.*, **260**, 838–848, (1982).

[181] Shibata, M., "Fully general relativistic simulation of coalescing binary neutron stars: Preparatory tests", *Phys. Rev. D*, (1999). For a related online version see: M. Shibata, "Fully general relativistic simulation of coalescing binary neutron stars: Preparatory tests", (August, 1999), http://xxx.lanl.gov/abs/gr-qc/9908027. in press.

[182] Shibata, M., and Nakamura, T., "Evolution of three-dimensional gravitational waves: Harmonic slicing case", *Phys. Rev. D*, **52**, 5428–5444, (1995).

[183] Shibata, M., W., Baumgarte. T., and Shapiro, S. L., "Stability of coalescing binary stars against gravitational collapse: hydrodynamical simulations", *Phys. Rev. D*, **58**, 023002, (1998). For a related online version see: M. Shibata, et al., "Stability of coalescing binary stars against gravitational collapse: hydrodynamical simulations", (May, 1998), http://xxx.lanl.gov/abs/gr-qc/9805026.

[184] Siegler, S., and Riffert, H., "Smoothed particle hydrodynamics simulations of ultra-relativistic shocks with artificial viscosity", (1999). For a related online version see: S. Siegler, et al., "Smoothed particle hydrodynamics simulations of ultra-relativistic shocks with artificial viscosity", (April, 1999), http://xxx.lanl.gov/abs/gr-qc/9904070. Submitted.

[185] Sloan, J., and Smarr, L. L., "General relativistic magnetohydrodynamics", in J. Centrella, J. LeBlanc, and Bowers, R., eds., *Numerical Astrophysics*, 52–68, (Jones and Bartlett, Boston, 1985).

[186] Smarr, L. L., *The structure of general relativity with a numerical illustration: the collision of two black holes*, PhD thesis, (University of Texas at Austin, 1975).

[187] Stark, R. F., "Non-axisymmetric rotating gravitational collapse and gravitational radiation", in C. R. Evans, L. S. Finn, and Hobill, D. W., eds., *Frontiers in numerical relativity*, 281–296, (Cambridge University Press, Cambridge, England, 1989).

[188] Stark, R. F., and Piran, T., "Gravitational-Wave Emission from Rotating Gravitational Collapse", *Phys. Rev. Lett.*, **55**, 891–894, (1985).

[189] Stark, R. F., and Piran, T., "A general relativistic code for rotating axisymmetric configurations and gravitational radiation: numerical methods and tests", *Comp. Phys. Rep.*, **5**, 221–264, (1987).

[190] Swesty, D., *Living Reviews in Relativity*, **2**, (1999). In preparation.

[191] Swesty, D., Lattimer, J. M., and Myra, E. S., "The role of the equation of state in the 'prompt' phase of type II supernovae", *Astrophys. J.*, **425**, 195–204, (1994).

[192] Tanaka, Y., and et al, "Gravitationally redshifted emission implying an accretion disk and massive black-hole in the active galaxy MCG:-6-30-15", *Nature*, **375**, 659–661, (1995).

[193] Teukolsky, S. A., "Rotating black holes: separable wave equations for gravitational and electromagnetic perturbations", *Phys. Rev. Lett.*, **29**, 1114–1118, (1972).

[194] Thorne, K., "Gravitational waves", in Kolb, E. W., and Peccei, R., eds., *Proceedings of the Snowmass 95 Summer Study on Particle and Nuclear Astrophysics and Cosmology*, (World Scientific, Singapore, 1996).

[195] van der Klis, M., "Kilohertz Quasi-Periodic Oscillations in Low-Mass X-Ray Binaries", in R. Buccheri, J. van Paradijs, and Alpar, M.A., eds., *Proceedings of the NATO Advanced Study Institute*, 337, (Kluwer Academic Publishers, Boston, 1998). For a related online version see: M. van der Klis, "Kilohertz Quasi-Periodic Oscillations in Low-Mass X-Ray Binaries - a Review", (October, 1997), http://xxx.lanl.gov/abs/astro-ph/9710016.

[196] van Leer, B. J., "Towards the ultimate conservative difference scheme. V. A second order sequel to Godunov's method", *J. Comput. Phys.*, **32**, 101–136, (1979).

[197] van Putten, M. H. P. M. For a related online version see: M. H. P. M. van Putten, "Uniqueness in MHD in divergence form: right nullvectors and well-posedness", (April, 1998), http://xxx.lanl.gov/abs/astro-ph/9804139.

[198] van Riper, K. A., "General relativistic hydrodynamics and the adiabatic collapse of stellar cores", *Astrophys. J.*, **232**, 558–571, (1979).

[199] van Riper, K. A., "Effects of nuclear equation of state on general relativistic stellar core collapse models", *Astrophys. J.*, **326**, 235–240, (1988).

[200] von Neumann, J., and Richtmyer, R. D, "A method for the numerical calculation of hydrodynamic shocks", *J. Appl. Phys.*, **21**, 232, (1950).

[201] Wen, L., Panaitescu, A., and Laguna, P., "A shock-patching code for ultrarelativistic fluid flows", *Astrophys. J.*, **486**, 919–927, (1997). For a related online version see: L. Wen, et al., "A shock-patching code for ultrarelativistic fluid flows", (December, 1996), http://xxx.lanl.gov/abs/astro-ph/9612045.

[202] Wilson, J. R., "A numerical study of gravitational stellar collapse", *Astrophys. J.*, **163**, 209–219, (1971).

[203] Wilson, J. R., "Numerical study of fluid flow in a Kerr space", *Astrophys. J.*, **173**, 431–438, (1972).

[204] Wilson, J. R., "A numerical method for relativistic hydrodynamics", in Smarr, L., ed., *Sources of Gravitational Radiation*, 275, (Cambridge University Press, Cambridge, England, 1979).

[205] Wilson, J. R, "Supernovae and post-collapse behaviour", in J. M. Centrella, J. M. LeBlanc, and Wilson, J. R., eds., *Numerical astrophysics*, 422–434, (Jones and Bartlett, Boston, 1985).

[206] Wilson, J. R., and Mathews, G. J., "Relativistic hydrodynamics", in C. R. Evans, L. S. Finn, and Hobill, D. W., eds., *Frontiers in numerical relativity*, 306–314, (Cambridge University Press, Cambridge, England, 1989).

[207] Wilson, J. R., and Mathews, G. J., "Instabilities in Close Neutron Star Binaries", *Phys. Rev. Lett.*, **75**, 4161–4164, (1995).

[208] Wilson, J. R., Mathews, G. J., and Marronetti, P., "Relativisitic Numerical Model for Close Neutron Star Binaries", *Phys. Rev. D*, **54**, 1317–1331, (1996). For a related online version see: J. R. Wilson, et al., "Relativisitic Numerical Model for Close Neutron Star Binaries", (January, 1996), http://xxx.lanl.gov/abs/gr-qc/9601017.

[209] Winicour, J., "Characteristic evolution and matching", *Living Reviews in Relativity*, **1**, (1998).

[210] Woodward, P., and Colella, P., "The numerical simulation of two-dimensional fluid flow with strong shocks", *J. Comput. Phys.*, **54**, 115–173, (1984).

[211] Woosley, S. E., "Gamma-ray bursts from stellar mass accretion disks around black holes", *Astrophys. J.*, **405**, 273–277, (1993).

[212] Woosley, S. E., Pinto, P. A., and Ensman, L., "Supernova 1987 A - Six weeks later", *Astrophys. J.*, **324**, 466–489, (1988).

[213] Yamada, S., "An implicit Lagrangian code for spherically symmetric general relativistic hydrodynamics with an approximate Riemann solver", *Astrophys. J.*, **475**, 720–739, (1997). For a related online version see: S. Yamada, "An implicit Lagrangian code for spherically symmetric general relativistic hydrodynamics with an approximate Riemann solver", (January, 1996), http://xxx.lanl.gov/abs/astro-ph/9601042.

[214] Yokosawa, M., "Energy and angular momentum transport in magneto-hydrodynamical accretion onto a rotating black hole", *Publ. Astron. Soc. Japan*, **45**, 207–218, (1993).

[215] Yokosawa, M., "Structure and dynamics of an accretion disk around a black hole", *Publ. Astron. Soc. Japan*, **47**, 605–615, (1995).

[216] York, J., "Kinematics and Dynamics of General Relativity", in Smarr, L., ed., *Sources of Gravitational Radiation*, (Cambridge University Press, Cambridge, England, 1979).

[217] Zampieri, L., Miller, J. C., and Turolla, R., "Time-dependent analysis of spherical accretion on to black holes", *Mon. Not. R. Astron. Soc.*, **281**, 1183–1196, (1996). For a related online version see: L. Zampieri, et al., "Time-dependent analysis of spherical accretion onto black holes", (July, 1996), http://xxx.lanl.gov/abs/astro-ph/9607030.